Mutant Tau knock-in mice display frontotemporal dementia relevant behaviour and histopathology

Koss, David J.; Robinson, Lianne; Drever, Benjamin D.; Plucińska, Kaja; Stoppelkamp, Sandra; Veselcic, Peter

Published in:
Neurobiology of Disease

DOI:
10.1016/j.nbd.2016.03.002

Publication date:
2016

Mutant Tau knock-in mice display frontotemporal dementia relevant behaviour and histopathology

*Dave J. Koss[1], *Lianne Robinson[1,2], Benjamin D. Drever[1], Kaja Plucińska[1], Sandra Stoppelkamp[1,3], Peter Veselcic[1,4], Gernot Riedel[1**] and Bettina Platt[1**]

*These authors contributed equally.

[1]School of Medical Sciences, University of Aberdeen, Foresterhill, Aberdeen, AB25 2ZD, UK.

[2] **current address:** Behavioural Neuroscience Core Facility, Division of Neuroscience, University of Dundee, Dundee, DD1 9SY, UK.

[3] **current address:** Dept. of Thoracic, Cardiac and Vascular Surgery, University Hospital Tübingen, Tübingen University, Calwerstr. 7/1, 72076 Tübingen, Germany.

[4] **current address:** AbbVie Germany GmbH & Co KG, Ludwigshafen, Germany.

**Joint corresponding authors:

Prof. Bettina Platt
School of Medical Sciences
College of Life Sciences and Medicine
University of Aberdeen
Institute of Medical Sciences
Foresterhill
Aberdeen AB25 2ZD
UK
Tel. +44 (0)1224 437402
Fax: +44 (0)1224 437465
Email: b.platt@abdn.ac.uk

Prof. Gernot Riedel
School of Medical Sciences
College of Life Sciences and Medicine
University of Aberdeen
Institute of Medical Sciences
Foresterhill
Aberdeen AB25 2ZD
UK
Tel.: +44 (0)1224 437377
FAX: +44 (0)1224 467465
email: g.riedel@abdn.ac.uk

Abstract

Models of Tau pathology related to frontotemporal dementia (FTD) are essential to determine underlying neurodegenerative pathologies and resulting Tauopathy relevant behavioural changes. However, existing models are often limited in their translational value due to Tau overexpression, and the frequent occurrence of motor deficits which prevent comprehensive behavioural assessments. In order to address these limitations, a forebrain-specific (CaMKIIα promoter), human mutated Tau ($hTau_{P301L+R406W}$) knock-in mouse was generated out of the previously characterised $PLB1_{Triple}$ mouse, and named $PLB2_{Tau}$. After confirmation of an additional hTau species (~60 kDa) in forebrain samples, we identified age-dependent progressive Tau phosphorylation which was coincided with the emergence of FTD relevant behavioural traits. In line with the non-cognitive symptomatology of FTD, $PLB2_{Tau}$ mice demonstrated early emerging (~ 6 months) phenotypes of heightened anxiety in the elevated plus maze, depressive/apathetic behaviour in a sucrose preference test and generally reduced exploratory activity in the absence of motor impairments. Investigations of cognitive performance indicated prominent dysfunctions in semantic memory, as assessed by social transmission of food preference, and in behavioural flexibility during spatial reversal learning in a homecage corner-learning task. Spatial learning was only mildly affected and task-specific, with impairments at 12-month of age in the corner learning but not in the water maze task. Electroencephalographic (EEG) investigations indicated a vigilance-stage specific loss of alpha power during wakefulness at both parietal and prefrontal recording sites, and site-specific EEG changes during non-rapid eye movement sleep (prefrontal) and rapid eye movement sleep (parietal). Further investigation of hippocampal electrophysiology conducted in slice preparations indicated a modest reduction in efficacy of synaptic transmission in the absence of altered synaptic plasticity.
Together, our data demonstrate that the transgenic $PLB2_{Tau}$ mouse model presents with a striking behavioural and physiological face validity relevant for FTD, driven by the low level expression of mutant FTD hTau.

Keywords: Frontotemporal Dementia, Tauopathies, Tau, phosphorylation, Cognition, Apathy, Anhedonia, Semantic memory, Spatial memory, EEG.

Highlights [3-5 bullet points]

- $PLB2_{Tau}$ mice express mutant human Tau without gross overexpression.
- Age-dependent Tau phosphorylation coincides with onset of behavioural deficits.
- Behavioural and emotional abnormalities are prominent, early occurring phenotypes.
- Robust semantic-like but subtle spatial memory impairments are evident.
- Reduced stage- and region-specific EEG changes and mild changes in hippocampal synaptic transmission were identified.

Introduction

The excessive phosphorylation and reduced microtubule (MT) association of the Tau protein leads to the formation of insoluble inclusions that are prominent cellular pathologies in many types of fronto-temporal dementia (FTD) (Goedert et al., 1988; Crowther, 1991). Tau gene mutations underlie ~5% of familial FTD cases with as many as 40% of all tauopathies, both sporadic and familial, presenting with Tau positive fronto-temporal lobar degeneration (see Neumann et al., 2009; Goedert et al., 2012 for reviews). Functionally, the majority of exonic FTD Tau variants leads to the promotion of phosphorylation, decreased phosphatase association, diminished MT binding and an increased propensity for protein self-aggregation (Goedert and Spillantini, 2000).

Despite a degree of shared common pathology between FTD tauopathies and Alzheimer's disease (AD), both dementias differ significantly in terms of early symptomatic presentation due to the divergent anatomical loci of neurodegeneration (Rabinovici et al., 2007). FTD can be broadly subdivided into behavioural variant FTD (bvFTD), associated with degeneration of the prefrontal cortex, and semantic variant FTD (svFTD), in which temporal lobe degeneration is primary (Ghosh and Lipp 2013). Although executive dysfunction is common in both, svFTD is associated with varying language-based deficits, whilst bvFTD manifests with altered emotionality, apathy, disinhibition and social withdrawal (see Mendez et al., 2008 for review). Early in FTD, memory and visuospatial abilities are relatively preserved (Hutchinson and Mathias, 2007). In contrast, AD emerges with pronounced deficits in memory and spatial abilities associated with degeneration of hippocampal areas and temporoparietal cortices (Rabinovici et al 2007); disruptions in executive function, language and mood are evident only following the spread of pathology. Though the symptomology of these dementias may converge as these diseases progress, it is clear that initial presentations and underlying pathological events are distinct.

Numerous human Tau (hTau) mouse models have been generated, exploiting the multitude of identified FTD *Tau* variants. These express hTau either alone (summarised in Table 1) or in combination with the AD relevant mutated genes, i.e. the human amyloid precursor protein (hAPP) and/or the Presenilin 1 (PS1) gene (Lewis et al., 2001; Oddo et al., 2003; Platt et al., 2011). The characterisation of early FTD transgenic lines was hindered by brainstem and spinal cord pathology and thus progressive motor deficits (see Lewis et al., 2000 and Allen et al., 2002 for example), but more recently region-specific promoters have somewhat overcome this limitation (Tatebayashi et al., 2002; Platt et al., 2011) allowing a more in-depth assessment of behaviour and cognition. It should be noted however that cortical-spinal neuronal loss and delayed motor impairments occurred in the Tg4510 model despite the use of the CaMKII forebrain specific promoter (Ramsden et al., 2005). Given the selection of transgene promoters, Tau isoforms and FTD variants, current models yield highly heterogeneous phenotypes (see Table 1).

As a consequence of the proportionally higher prevalence of AD, mouse lines have been preferentially designed for robust hippocampal transgene expression and often report deficits within hippocampus-dependent learning. Only few models have been thoroughly investigated for non-cognitive aspects such as altered emotionality and disinhibition, more akin to the early symptomatic presentation reported in human FTD cases (Takeuchi et al. 2011; Van der Jeugd 2013).

Interestingly, several models with relatively low transgene expression (0.1-2 fold increase), such as a V337M model (Tamemura et al., 2001) as well as our recently published line 66 (L66) mouse model (Melis et al., 2015) are without deficits in spatial learning despite evident tau pathology. The preservation of basic hippocampal function was also recently observed in a non-transgenic rat model of FTD, where the intra-hippocampal delivery of recombinant hTau induced cognitive impairments related to cognitive flexibility rather than spatial memory (Koss et al., 2015). In contrast, the selective expression of mutant hTau within the entorhinal cortex (de Calignon et al., 2012) or the expression of paired helical filament derived Tau truncation products (Hrnkova et al., 2007; Line 1 in Melis et al., 2015) appears to preferentially engage AD relevant pathological mechanisms, recapitulating Braak stage progression of tau pathology and selectively affecting spatial (hippocampal) aspects over those underlying emotional processing and motor function. Thus, dependent on variables such as the tau species and level of expression, differential pathological processes and regional effects may occur which align phenotypes with the symptomology of AD vs. FTD.

Determining the underlying variables instrumental to such diversity in existing tau models has somewhat been hindered. Critical drawbacks relate to pronuclear transgene technologies, which results in the integration of multiple gene copies at random sites within the genome; this can lead to transgenic mutagenesis and endogenous gene silencing. The gross overexpression of transgenes further complicates the inference of pathophysiological mechanisms (Gama Sosa et al., 2010): Tau overexpression ranged between 1-13 fold over endogenous levels, which is problematic given that the expression of wild-type hTau also induced clear histological and behavioural pathology (Spittaels et al., 1999, Polydoro et al., 2009), as pathogenic mechanisms engaged by mutated vs. non-mutated hTau variants are likely distinct (Furukawa et al., 2003, Khandelwal et al., 2012). However, initial attempts to generate a knock-in FTD mouse model failed to generate overt Tau phospho-pathology and the associated behavioural deficits even up to 32 months of age (Gilley et al., 2012). The absence of pathology may potentially be a consequence of the insertion of a mutant analogue (P290L rather than P301L) into the murine Tau gene. Beyond these concerns, cross-model comparison is further complicated by variable background strains, which influence phenotypes of emotionality (Podhorna and Brown, 2002; Salomons et al., 2012) cognition (Brooks et al., 2005), and potentially key features

such as phosphorylation, inflammation and neurodegeneration (Stozicka et al., 2010; Bailey et al., 2014).

Here, we characterise the $PLB2_{Tau}$ knock-in mouse, which expresses a single copy of FTD hTau (2N4R TauP301L + R406W) alongside endogenous murine Tau. The phenotypic characterisation comprised not only Tau pathology and assessment of learning and memory performance, but also non-cognitive behaviours such as anxiety, hedonia, motor activity and exploration alongside vigilance staging and electrophysiological measurements.

Methods

Animals

Mice were housed and tested in accordance with UK Home Office regulations. All experimental procedures were subject to the University of Aberdeen's Ethics Board and conducted in accordance with the European Directive on the Protection of Animals used for Scientific Purposes (2010/63/EU) and the Animal (Scientific Procedures) Act 1986. Mice were bred at a commercial vendor (Harlan, UK) and delivered to the local facility 2-3 weeks prior to testing. All mice were housed in a climate -maintained (temperature 23±2^{o}C and relative humidity 40-60%) holding room under a 12 hour light/dark cycle (lights on 7 am; lights off 7 pm), with food and water provided *ad libitum.*

$PLB2_{Tau}$ mice were generated by crossing of the previously described heterozygous $PLB1_{Double}$ female mice (Platt et al., 2011; Calamai et al., 2013) with heterozygous Cre-recombinase expressing male mice. $PLB1_{Double}$ mice (C57BL6/J background strain) expressed a single human *APP-Tau* (h$APP_{770Lon(V717I)+Swe(KM670/671NL)}$ / 2N4R h$Tau_{P301L+R406W}$) gene construct regulated by the murine Ca^{2+}/Calmodulin-dependent Kinase IIα (CaMKIIα) promoter inserted via targeted knock-in into the HPRT genomic locus (Fig. 1A). *hAPP* and *hTau* transgenes within the construct were flanked by LoxP and FRT recognition sites, respectively. Accordingly, the progeny from the breeding of $PLB1_{Double}$ X Cre-recombinase mice were either wild-type, $PLB1_{Double}$ mice expressing the full *APP-Tau* gene construct or expressed only the *Tau* gene (Fig 1.B), referred to throughout the manuscript as $PLB2_{Tau}$ mice. Wild-type (PLB_{WT}) mice were derived from a parallel PLB_{WT} line (as described in Platt et al., 2011).

Validation of APP Gene Excision and Routine Genotyping of Transgenic Mice

Genomic DNA isolated from ear biopsies were screened for transgene expression by means of PCR amplification with a modified HPRT primer set (Forward: 5'-CACTAGCCGTTACCATAGCAACTGC-3'and Reverse: 5'-GCAGTAGCCTCATCATCACTAGATGG-3'). Determination of successful *hAPP* excision and thus identification of $PLB2_{Tau}$ mice was achieved by size comparison of the PCR amplification product, i.e. $PLB1_{Double}$ mice produced a product of ~ 5.6 Kb, whereas $PLB2_{Tau}$ mice expressing only *hTau* produced a product of 2.6 Kb (Fig 1.B).

hTau regional gene expression

$PLB2_{Tau}$ transgene expression was confirmed by quantitative PCR (Platt et al., 2011). In brief, forebrain and cerebellum samples from 12-month old PLB_{WT} and $PLB2_{Tau}$ mice (n=5 for both) were treated as per manufactures guideline using the RNeasy lipid tissue mini kit (Qiagen). RNA samples were controlled for integrity (Agilent 2100 bioanalyzer, Cheshire, UK, RIN-score>7) before cDNA was synthesised with the Transcriptor High Fidelity reverse transcriptase kit (Roche, Burgess Hill, UK). The cDNA (100 ng) was run in triplicate with 3.2 µM *hTau* transgene specific (Forward: 5'-CACGGACGCTGGCCTGAAAG-3', Reverse: 5'-CTGTGGTTCCTTCTGGGATC-3') and *GAPDH* housekeeping gene specific (Forward: 5'-ACTTTGTCAAGCTCATTTCC-3', Reverse: 5'-TGCAGCGAACTTTATTGATC-3') primers using a BioRad miniOpticon real-Time PCR detection system with iQ SYBR green supermix (Biorad Hemel Hempstead, UK). Data analysis was performed using the Opticon monitor TM software (Biorad); gene expression values were quantified relative to endogenous *GAPDH* housekeeping gene values. Due to the low transgene expression (cf. *GAPDH*), normalised values were multiplied by a factor of 10^4, to allow for graphic representation. Regional brain expression was assessed by two-tailed Student's t-test comparison.

Tau protein expression and phosphorylation

Mice were sacrificed by cervical neck dislocation, brains snap frozen in liquid nitrogen and stored at -80 ^{O}C. For soluble protein quantification, hemi-forebrain samples (For hTau expression n=6 for 6m PLB_{WT} and $PLB2_{Tau}$ mice and n= 5 for 12m PLB_{WT} and $PLB2_{Tau}$ mice; for total Tau and phospho-Tau PHF-1 and CP-13, n=14, 12, 12 and 16 for 6-month old PLB_{WT}, $PLB2_{Tau}$, 12-month old PLB_{WT} and $PLB2_{Tau}$ mice) were homogenised in ~1:10 (W/V) Igepal lysis buffer (in mM: 20 HEPES, 150 NaCl, 0.1 EDTA, 1% Igepal: pH=7.6), containing complete protease inhibitors (Roche) and PhosStop tablets (Roche), then spun at 4^{O}C for 20 mins at 12000 revolutions per minute (rpm) and the supernatant separated from pellet. The resulting supernatant was additionally heated at 90 ^{O}C for 10 mins, spun (10 mins, 14000 rpm at 4 ^{o}C) and the Tau-enriched heat-stable fraction isolated (modified from Petry et al., 2014).

Heat-stable fractions were adjusted for protein content as established by a bicinchoninic acid (BCA) colourmetic protein assay (Sigma, Dorset, UK) before mixing with lithium dodecyl sulfate (LDS) loading buffer containing 15 mM dithiothreitol (DTT). Samples were boiled at 70^{o}C for 10 mins, separated on 4-12 % Bis-Tris Nupage gels (Invitrogen, Paisley, UK), immunoblotted on 0.45 µm pore nitrocellulose membranes. Membranes were blocked for 1 hr in Tris-buffered saline with Tween (TBST: in mM 50 Trizma base, 150 NaCl, 0.5% Tween-20), containing 5 % bovine serum albumin or 5 % milk powder for phospho and non-phospho sensitive antibodies, respectively. Membranes were incubated overnight (4^{o}C) in primary antibodies (HT-7, Pierce, AT-5, Abcam, AT-8, ThermoFisher Scientific, PHF-1 and CP-13, generous gifts from Prof. P. Davies) and for 1 hr in secondary antibody (goat-anti mouse, Millipore, 1:5000) at room temperature. Western blots were visualised via enhanced chemiluminescent substrate (Tris-HCl, 1.25 mM luminol, 30 µM coumaric acid, 0.015 % H_2O_2) and captured with a Vilber-Fusion camera (Fusion Spectra software FX).

For insoluble-enriched fractions, pellets were homogenised twice in Igepal lysis buffer (1ml), spun at 14000 rpm for 20 mins at 4^{o}C, supernatants discarded, prior to incubation of remaining pellet overnight at 4 ^{o}C, in 1:1 (W/V) 70 % formic acid (Sigma). Following incubation, samples were again spun at 14000 rpm for 20 mins at 4 ^{o}C, before the supernatant was collected and neutralised with 4x neutralising buffer (2 M Tris + 2 M NaH_2PO_4) and treated as above with LDS and DTT and boiling.

Densitometric blot analysis was conducted using 16 bit image analysis with ImageJ; quantification for each sample was normalised for protein loading by re-probing membranes for total Tau as detected by the AT-5 pan Tau antibody (1:5000, Abcam). Values were normalised cf. PLB_{WT} and pooled for each genotype (PLB_{WT} or $PLB2_{Tau}$). Statistical significance was established via 2-tailed Student's t-tests between selected data pairs.

Behavioural characterisation

Unless stated, all cohorts used for behavioural tests were of mixed gender and genotypes, and closely matched for age (±4 weeks).

Spatial Learning (Open Field Water Maze)

Spatial learning was investigated in PLB_{WT} (6-month: n=19, 12-month old: n=14), and $PLB2_{Tau}$ (6-month: n=19, 12-month: n=16) mice with the well-established open field water maze (WM) paradigm (see Platt et al., 2011; Ryan et al., 2013; Plucińska et al., 2014). Using a white Perspex water filled pool (150 cm diameter, 50 cm in height, water temp 21±1^{o}C), animals were allocated a fixed platform position (rising platform, Ugo Basile, Varese, Italy) and released from one of four sites along the edge of the pool, (N,E,S,W) in pseudo-random fashion. Initially, all mice performed a 1 day visible platform test with curtains drawn around the pool to obscure spatial cues (4 trials, 90 sec maximum trial duration, 30

min inter trial interval (ITI)) to ensure that mice had intact visual ability. This was followed by 4 days of spatial reference training to a submerged platform (4 trials per day, 90 sec maximum swim duration, 30 min ITI, no curtains). A probe trial (60 sec duration, no platform) was performed 1 hr post acquisition. Swim paths of all trials were recorded via an overhead camera and Any-Maze tracking software (Ugo Basile). Path length and swim speed were analysed for visible and spatial learning trials and time in pool quadrants for probe trial. Mean path lengths per training day were compared via a 2-way repeated measures ANOVA (day and genotype as variables) and the probe trial analysed via one sample t-tests comparing mean % time in target quadrant to chance level (25 %).

Spatial Corner Learning (IntelliCage)

The spatial learning abilities were further determined using the IntelliCage system (New Behavior, TSE-Systems Bad Homburg, Germany) as previously described (Ryan et al., 2013; Robinson and Riedel, 2014). Female mice, 6 (PLB_{WT}: n=10 and $PLB2_{Tau}$: n=10) and 12-month old (PLB_{WT}: n=15 and $PLB2_{Tau}$: n=13) were implanted with a unique radio transmitting microchip (Planet ID, New Behaviour) which enabled tracking and identification of individuals as they entered the experimental corners. Mice were given a 2 day habituation period, during which water was available in all corners. The number of visits to each corner was recorded for each mouse, thus establishing baseline corner visiting behaviour and any pre-training corner preference. During the 12 hr test period (conducted in the dark phase), individuals were assigned a single corner in which water could be obtained, all other corners could be entered but water was not available. By monitoring the specific corner visits of each mouse, relative to total corner visits over the 12 hr time period, learning of spatial location for water access was quantified. In 6-month old PLB_{WT} and $PLB2_{Tau}$, a reversal learning paradigm was conducted following spatial learning, whereby the spatial location of the water supplying corner was switched to the opposite corner for a 12 hr test period and corner visitations recorded. Learning was determined by one sample t-test of % corner visits to the hypothetical chance value (25 %) for each genotype. Additionally two tailed Student's t-test comparisons were conducted between genotypes.

Social Transmission of Food Preference

Prior to testing, all mice were evaluated for intact basic olfaction using a buried cookie test (see Plucińska et al., 2014 for details). For social transmission of food preference (STFP), a food bias was induced in an "observer" mouse via a social interaction with a "demonstrator" mouse (previously, exposed to the cued food). This test of olfaction-based semantic-like memory, was conducted with 6-month old PLB_{WT}, and $PLB2_{Tau}$ mice (n=21 and 13, respectively). The paradigm consisted of 4 sequential phases: i) Habituation (3 days within PhenoTyper cages, water and food *ad libitum*), ii) assessment of food jar spatial location preference (24 hr period), iii) social interaction (SI) with the demonstrator mouse and iv) memory test. Prior to SI all mice were food deprived for 16 hrs. Demonstrator mice

were exposed to cued food flavours (1 % cinnamon or 2 % cocoa) for 30 mins, before being placed in SI cylinders within the observer's cage for 30 mins. SI activity was monitored (time spent within a pre-determined interaction zone). Following the SI phase, demonstrator mice were removed and after a delay of 15 mins (short-term memory test: STM) and 24 hrs (long-term memory test: LTM), the observer mice were presented with two food jars (cued and novel). Principle measurements of food intake (in grams) for correct and incorrect preference were calculated for both STM (duration: 30 min) and LTM (duration: 16 hr). A significant bias for cued food flavour (% cued food) was taken as an index of intact semantic-like memory. Comparison of food intake (correct vs. incorrect and between genotypes) was conducted via two tailed Student's t-tests and food bias determined by comparison of food preference to chance level (50%) via a one sample t-test.

Elevated Plus Maze

Assessment of anxiety in 6-month old PLB_{WT} (n=14) and $PLB2_{Tau}$ (n=10) mice was performed using the elevated plus maze (EPM) as described by Plucińska et al. (2014). Briefly, mice were placed into the central area of the maze (42 cm elevated grey cross-shaped Perspex apparatus; arms: 35 cm long × 5 cm wide; central square: 5 × 5 cm, closed arms enclosed by vertical walls and open arms with unprotected edges). Time spent within the three zones of the arena (open arms, closed arms and centre) during a 5 min exploration period was recorded by an overhead camera using Ethovision (V3.1 Plus) tracking software (Noldus IT, Wageningen, Netherlands). Comparisons between genotypes were made using two tailed Student's t-tests. Time spent in closed arms of the arena was used as an index of anxiety.

Sucrose Preference Task (IntelliCage)

Pleasure-seeking behaviour (hedonia) was evaluated in 6-month old PLB_{WT} and $PLB2_{Tau}$ female mice (n=10 for both) by a sucrose preference task conducted in the IntelliCage system. Mice, implanted with microchips (as in spatial corner learning), were habituated to the IntelliCage for 2 days (water available in all corners), followed by 3 test days where water could be obtained from two corners and a 1% sucrose solution was available in the other two corners. The number of entries and licks performed in the sucrose and water corners was taken as a measure of preference. Bias for sucrose corner visits/licks were assessed by comparing sucrose offering corner visits (%) to chance level (50%, one sample t-test). Further genotype differences were probed via a 2-way repeated measures ANOVA (day and genotype as variables for corner visits and licks and genotype as variables for mean licks over the 3 day test period).

Motor Coordination

The sensory motor coordination of 14-month old PLB_{WT} and $PLB2_{Tau}$ cohorts was tested using the balance beam as previously described (Robinson et al., 2013). PLB_{WT} (n=12) and $PLB2_{Tau}$ (n=13) mice were tested for latency to traverse beams of varying diameter (28, 11 or 5 mm) and shape (square or round). All beams were 50 cm in length with a 30% incline. Each mouse was given two trials per beam (maximum duration 30 sec) and the latency to reach the top end was averaged. Differences in motor coordination for squared or rounded beams were established via 2-way repeated measures ANOVAs, with genotype and beam diameter as variables; post-hoc Bonferroni tests compared the genotype performance at individual beam diameters.

Activity and Circadian Rhythm

Using the PhenoTyper homecage system (Noldus IT, Wageningen, Netherlands), parameters relating to novel environment habituation, exploratory behaviour and circadian activity patterns were measured in 6-month old mice (PLB_{WT} n=12, $PLB2_{Tau}$ n=13), as previously described (Robinson et al., 2013; Plucińska et al., 2014). Mice were singly housed and given 2 days of habituation prior to assessment of circadian activity (days 3 -7). Novel environment habitation was measured as distance moved (extracted in 10min bins) for the initial 3hrs following placement in the PhenoTyper. Over the following experimental days, distance moved was extracted (in 1 hr bins) across all days to determine exploratory and circadian phasic activity over the 24 hr cycle and 12 hr light-dark periods. Habituation data were fitted for one-decay non-linear regression analysis. Comparison of fit was first employed to determine significant differences, before individual comparisons of the initial activity levels (Y0), activity decay rate (K) and post-habituation activity (plateau) were performed. All data from the subsequent 4 day recording period was probed for significant differences by means of repeated measures 2 way ANOVA with genotype and time as variables.

Electroencephalogram (EEG) assessments

A subset of mice (6-month old PLB_{WT} n=6 and $PLB2_{Tau}$ n=5) underwent surface EEG recordings during the PhenoTyper paradigm as described previously (Platt et al., 2011; Jyoti et al., 2015). Mice were implanted with epidural electrodes above the left and right parietal cortex/dorsal hippocampus (mm relative to Bregma; anterior-posterior axis: +2, medial-lateral axis: ±1.5), the right medial prefrontal cortex (mm relative to Bregma; anterior-posterior axis: +2, medial-lateral axis: +0.2) and reference/ground electrodes placed at neutral locations. Following post-surgery recovery, a 24 hr EEG recording was captured via a wireless EEG device (Neurologger, New Behaviour, Switzerland) on the 3rd day of home cage activity recorded in the PhenoTyper (200 Hz sampling, band pass filters: high pass: 0.25 Hz, low pass: 70 Hz). Animal movement was detected via a built-in accelerometer. All data were exported to a PC and converted using EEG Process (Matlab 7, The MathWorks Inc., Natick, USA) before imported into SleepSign (Kissei Comtec Co. Ltd,

Nagano, Japan) for analysis of vigilance staging (Wakefulness (wake), REM and NREM sleep) and power spectra extrapolation (from 4 sec epochs). EEG spectra were determined using Fast Fourier Transform (FFT; 0.77 Hz resolution, Hamming window smoothing), averaged and normalised to peak as in previous studies (Platt et al., 2011; Jyoti et al., 2015). For vigilance staging, spectral EEG characteristics of each epoch were classified as NREM, REM or wake based on accelerometer activity and parietal/hippocampal spectral power (delta and theta power). Time spent in different vigilance stages were calculated (in %) during a 4hr diurnal (sleep phase: 10:00-14:00hrs) and nocturnal (activity phase: 22:00-02:00hrs) period. Statistical comparison employed two way ANOVAs (with state and genotype as variables for vigilance stage and genotype and spectral bands as variables for power spectra), individual comparisons between genotypes were evaluated by post-hoc Bonferroni tests. Spectral bands were defined and illustrated as delta (δ; 1.5–5 Hz), theta (θ; 5–9 Hz), alpha (α; 9–14 Hz), beta (β; 14–20 Hz) and gamma (γ; 20–30 Hz).

Hippocampal Slice Electrophysiology

Slice preparation and electrophysiological recordings were made as previously reported (Platt et al., 2011; Koss et al., 2013). In brief, terminally anaesthetised PLB_{WT} and $PLB2_{Tau}$ mice (6, 12 and 24-month old) were decapitated, brains removed and hippocampi dissected in ice cold sucrose-based artificial cerebrospinal fluid (aCSF, mM: 249.2 sucrose, 1.5 KCl, 1.3 $MgSO_4$, 0.96 $CaCl_2$, 1.5 KH_2PO_4, 2.89$MgCl_2 \cdot 6H_2O$, 25 $NaHCO_3$ and 10 glucose, pH 7.4, gassed with 95% O_2 / 5% CO_2). Hippocampal slices (400 µm) were stored for at least 1 hr before use in oxygenated, 32^{o}C, standard aCSF (composition as above, except the replacement of sucrose with 129.5 mM NaCl and increased $CaCl_2$ concentration of 2.5 mM). CA1 field excitatory postsynaptic potentials (fEPSPs) were stimulated by monopolar stimulation electrodes (WPI, UK, 0.5 MΩ) positioned in the Schaffer collateral/commissural fibres and recorded from the stratum radiatum via aCSF filled borosilicate glass electrodes (3-7 MΩ). Captured signals were amplified by a CV203BU preamplifing headstage (gain of 1, Axon Instruments) and an Axoclamp 200B amplifier (Axon Instruments), before being digitized (CED 1401 Plus, Cambridge Electronic Design, Cambridge, UK) and acquired with a PC running P-WIN software (Leibniz Institute for Neurobiology, Magdeburg, Germany). For the generation of input/output curves (I/O) of basal synaptic transmission, stimulation intensity was increased stepwise, until field excitatory post-synaptic potential (fEPSP) saturation was achieved (2.5-40 V; 2.5 V increments). For long term potentiation (LTP) experiments, baseline recordings (stimulation intensity: 40-50 % of fEPSP maximum, 30 sec inter-stimulus interval) were made for 10 mins prior to theta burst tetanus stimulation (5 Hz, five bursts of four stimuli, 100 Hz, inter burst interval: 200 ms for 1 second) which was followed by 60 mins of post tetanus stimulation/recordings (as for baseline recordings). Only slices that showed a variability of < 10% in baseline recordings were used. For long term depression (LTD), the induction was based on a low frequency stimulation protocol (900 pulses at 1 Hz). Measurements of presynaptic release and short-term plasticity were

also assessed using a paired-pulse protocol (stimulation intensity: 60% of EPSP saturation inter-stimulus intervals: 10, 20, 40, 100 and 200 ms).

For I/O curves, fEPSP slopes were pooled for genotype and age, expressed as mean values and plotted against stimulus intensity (PLB_{WT}: n=37, 40 and 40. $PLB2_{Tau}$: n=26, 45 and 31 for 6, 12 and 24-months of age, respectively) as well as against pre-synaptic fibre volley (PLB_{WT}: n=11, 10 and 18. $PLB2_{Tau}$: n=11, 16 and 18 for 6, 12 and 24-months of age). Long-term plasticity in hippocampal slices (LTP: PLB_{WT}: n=23, 17 and 11. $PLB2_{Tau}$: n=8, 25 and 10, for 6, 12 and 24 months of age and LTD at 12 and 24-months of age, n=10 for both age and genotype groups) signals were expressed relative to baseline values and mean values probed for differences in post tetanus time course between groups. For paired-pulse responses (PLB_{WT}: n=9, 16 and 14. $PLB2_{Tau}$: n=10, 14 and 9 for 6, 12 and 24-months of age, respectively), the second response was calculated relative to the first response (S2/S1). Comparisons between groups were made via 2-way ANOVA (genotype/age and stimulus/pre-synaptic fibre volley, as variables) for input/ output fEPSP slopes. Post tetanus changes were compared via 2-way repeated measures ANOVA (genotype/age and time as variables).

Data Analysis

Prism Software (V.5 GraphPad, CA, USA) was used for all statistical analyses and data are expressed as means + or ± SEM. α was set at 0.05, with $p<0.05$ being considered statistically significant, $p<0.01$ as highly significant and $p<0.001$ as extremely significant.

Results

Confirmation of Construct Expression

Founder $PLB2_{Tau}$ mice were derived from selective cross-breeding of homozygous PLB_{Double} female mice with heterozygous Cre-recombinase expressing male mice. Successful genomic excision of the LoxP-flanked *hAPP* gene was confirmed in the resulting offspring via ear biopsy PCR with a modified HPRT primer set (see methods). Mice expressing only the *hTau* transgene were identified by the production of a 2.6 kb amplification product in contrast to the 5.6 kb amplification product derived from the expression of the non-excised PLB construct (Fig. 1.A+B). Mice identified as hemizygous $PLB2_{Tau}$ males and heterozygous $PLB2_{Tau}$ females were then crossed to produce a homozygous line for subsequent breeding. All further analysis was conducted on homozygous / hemizygous offspring.

The regional transgene specificity provided by the CaMKIIα promoter was confirmed in 12-month old $PLB2_{Tau}$ mice via quantitative PCR (Fig. 1.C). Forebrain samples, probed with *hTau* specific primers, yielded a ~10 fold increase in PCR product levels over those

detected in cerebellum samples from the same mice ($p<0.001$, n=5). No amplification product was detected in PLB_{WT} samples. Transgene expression was ~24-fold below that of endogenous murine Tau levels, established in PLB_{WT} mice ($p<0.001$, data not shown).

hTau Protein Expression and Tau phosphorylation

Forebrain tissue analysis confirmed the expression of FTD mutant hTau. Despite the low RNA yield of the $PLB2_{Tau}$ transgene, hTau protein was robustly detected in heat-stable extracts in samples from 6- and 12-month old $PLB2_{Tau}$ mice (HT-7 immunoreactive band migrating at 60kDa, Fig. 2.A+B). No corresponding immunoreactive signal was observed in any of the PLB_{WT} samples. Comparison between 6- and 12-month old $PLB2_{Tau}$ samples suggested a relative reduction in the abundance of hTau in the soluble fraction of forebrain lysates with age (Fig 2.B, $p=0.07$, respectively). Overall Tau protein expression (pooled pan Tau AT-5 immunoreactive bands, corresponding to ~50 kDa: 0N4R, ~55 kDa: 1N4R and ~60 kDa: 2N4R adult Tau isoforms, McMillan et al., 2008), was not altered relative to age-matched controls at 6 or 12-months of age (Fig. 2.A+C, $p>0.05$), likely due to the unaltered levels of the major 50 kDa species. When considered independently, modest but significant increases in levels of 55 and 60 kDa Tau species were observed in $PLB2_{Tau}$ mice at 6- and 12-months of age (Fig. 2.A+D+E). Together, the data verify the successful expression of the *hTau* transgene in $PLB2_{Tau}$ mice and further demonstrate an increase of endogenous murine Tau (55 kDa band). Preliminary investigations into the levels of insoluble Tau with matching samples suggested no difference between genotypes (data not shown).

Enhanced Tau phosphorylation at the PHF-1 epitope (Ser396/Ser404) was observed in brain lysates from 6-month (Fig. 3.A+B, $p<0.01$) and 12-month old $PLB2_{Tau}$ mice (Fig. 3.A+B, $p<0.001$) relative to corresponding PLB_{WT} samples when tested at 7.5 µg protein/lane. Further analysis of the individual bands demonstrated an age-dependent progression of phosphorylation at the PHF-1 epitope in the $PLB2_{Tau}$ mice, such that at 6-months of age, only the 50 (Fig. 3.C, $p<0.01$) and 55 kDa (Fig. 3.C; $p<0.05$) phospho-Tau species were elevated (Fig. 3.A+C), yet by 12-months of age, all Tau species demonstrated robust increases (Fig. 3.A +D, $p<0.05$). Similar changes in Tau phosphorylation were observed for the CP-13 (Ser202) epitope, when pooled (Fig. 3.E +F) or as individual Tau species (Fig. 3.E+G+H). Additionally, a subtle but significant increase in the phospho-epitope AT-8 signal was observed for both 6 and 12-month old $PLB2_{Tau}$ samples (Fig 3.I; $p<0.05$ and $p<0.01$ for 6 and 12 month old $PLB2_{Tau}$ samples respectively). Note that 15 µg as oppose to 7.5 µg of protein per lane was required in order to visualise all tau immunoreactive bands. As for the previous epitopes, the 50 kDa migrating band was elevated at 6 months of age relative to PLB_{WT} samples (Fig 3.K; $p<0.05$) and increased 60 kDa immunoreactivity emerged by 12-months of age (Fig 3.L; $p<0.05$).

1) Behavioural characterisation: *Learning and memory*

a) Spatial Reference Memory: Open Field Water Maze

Assessment of spatial learning and memory was initially conducted in the established hippocampus-dependent water maze (WM) paradigm. Intact visual acuity was confirmed in $PLB2_{Tau}$ mice; no effect of age or genotype were observed during the visible platform test ($p>0.05$, data not shown). Spatial acquisition in $PLB2_{Tau}$ mice at either 6 or 12-months of age was intact (Fig. 4.A+D, genotype effect: $p>0.05$ for both age groups), and neither genotype presented with age-related changes ($p>0.05$). Only accelerated swim speeds compared with PLB_{WT} mice were observed at 12-months (Fig. 4.D, $PLB2_{Tau}$: $F_{(1,112)}=25.56$, $p<0.001$) but not at 6-months of age (Fig. 4.B). In agreement with acquisition performance, spatial retention during probe trials indicated that all groups displayed a preference for the trained quadrant (Fig. 4.C+F, $p<0.05$ cf. chance, for all).

b) Corner Learning and Reversal

Spatial learning and memory was further probed in the Intellicage via a water rewarded corner learning paradigm. At 6-month of age, PLB_{WT} mice acquired a preference for the water corner during the spatial learning (Fig. 5.A, $p<0.05$ cf. chance). In contrast, $PLB2_{Tau}$ failed to attain a spatial bias ($p=0.05$ cf. chance). Notably, comparison of total corner visits performed by each group across the habituation and test phases indicated a prominent hypo-active phenotype in the $PLB2_{Tau}$ mice (Fig. 5.B: $F_{(1,18)}=10.02$, $p<0.01$).

The 6-month cohort was further tested in a reversal learning paradigm. Both groups displayed a significant corner preference above chance (Fig. 5.A, $PLB_{WT}=47.7\pm2.7\%$ $p<0.001$ and $PLB2_{Tau}=35\pm4.2\%$, $p<0.05$), however $PLB2_{Tau}$ mice displayed a reduced preference for the reversal corner relative to controls ($p<0.05$). In addition, a trend towards a hypoactive phenotype in the $PLB2_{Tau}$ mice was again observed (fewer total corner visits compared to controls; Fig. 5.B, $p=0.06$).

At 12-months of age $PLB2_{Tau}$ mice demonstrated a clear impairment in spatial learning and failed to acquire a preference for the water corner (Fig. 5.C, $PLB2_{Tau}$; $p>0.05$, cf. chance). The performance of PLB_{WT} mice was unaffected by age (corner preference $p<0.001$, cf. chance; effect of age $p>0.05$). Similar to observations at 6-month of age, $PLB2_{Tau}$ mice continued to display hypoactivity with a reduced number of total corner visits (Fig. 5.D, genotype effect $p<0.05$).

c) Social Transmission of Food Preference

Next, semantic-like memory of 6-month old PLB_{WT} and $PLB2_{Tau}$ mice was assessed. As STFP is dependent on olfaction and social motivation, all mice were initially evaluated for comparable performances in the cookie test and SI phase of the STFP paradigm. No

significant genotype effect was observed in the cookie test ($p>0.05$, data not shown) or during the SI phase (time spent in proximity of demonstrator mouse, $p>0.05$, data not shown). A robust preference for the correct (cued) food was detected in PLB_{WT} mice following a 15 min delay (Fig. 6.A, STM; $p<0.01$) and 24 hr delay (Fig. 6.A, LTM; $p<0.001$). In contrast $PLB2_{Tau}$ mice failed to display such a preference independent delay (Fig. 6.A, $p>0.05$ for both STM and LTM) and consumed less of the correct food ($PLB2_{Tau}$ cf. wild-type mice: $p<0.05$ and $p<0.001$ for STM and LTM, respectively). Total food intake during either of the test phases was not different between genotypes ($p>0.05$ for all, data not shown). The semantic memory impairment was further confirmed when food preference was considered as % of total intake (Fig. 6.B, PLB_{WT} $p<0.001$ cf. 50% chance for STM and LTM, $PLB2_{Tau}$: $p>0.05$ cf. chance for STM and LTM).

2) Non-cognitive Phenotypes

a) Anxiety

In addition to memory impairments, FTD often presents with a range of emotional alterations. Anxiety was investigated at 6 months of age using the EPM in PLB_{WT} and $PLB2_{Tau}$ mice. The EPM was highly anxiogenic independent of genotype; all mice spent the vast majority of time in the closed arms of the maze (Fig. 7.A, 84.9±2.4 % for PLB_{WT} and 91.6±1.3 % for $PLB2_{Tau}$ mice). A slight, yet significant increase in time spent in the closed arms was observed in $PLB2_{Tau}$ mice, alongside a corresponding reduction in the time spent exploring the open arms of the maze ($p<0.05$).

b) Anhedonia

Additional 6-month old cohorts were tested for pleasure seeking behaviour (hedonia) by exploiting the natural preference of mice for sweet food sources. When analysed over the entire 72 hr observation period both PLB_{WT} and $PLB2_{Tau}$ mice displayed a strong preference for visiting sucrose corners over those containing water ($p<0.001$, cf. chance level); however, the overall preference for sucrose corners was reduced in $PLB2_{Tau}$ mice. Initially, $PLB2_{Tau}$ mice demonstrated no preference, but gained preference for the sucrose corner from day 2 (Fig. 7.Bi, Day 1: $p>0.05$, day 2: $p<0.05$, day 3: $p<0.001$). In contrast, PLB_{WT} mice strongly opted for the sweetened water across all experimental days. Correspondingly, an effect of genotype ($F(1,36)=14.55$, $p<0.01$), day ($F_{(2,36)}=3.771$, $p<0.05$) and an interaction ($F_{(2,36)}=19.8$, $P<0.001$) were observed. Sucrose preference was further corroborated by the number of licks (Fig. 7.B ii) with an effect of drinking solution ($F_{(1,18)}=541.3$; $p<0.001$) and an interaction with genotype and drinking solution ($F_{(1,18)}=22.76$; $p<0.001$). PLB_{WT} and $PLB2_{Tau}$ mice displayed a greater number of licks in the sucrose corner compared to chance ($p<0.001$ for both). However, $PLB2_{Tau}$ mice licked less cf. controls in the sucrose corner and more in corners containing water ($p<0.001$). Fewer total visits in the $PLB2_{Tau}$ mice compared to PLB_{WT} were recorded, which again suggests a

hypo-active phenotype at 6-months of age; yet this did not reach significance (genotype effect: p=0.07).

3) Movement, Exploration and Vigilance

a) Motor Coordination

The reduced number of corner visits performed by $PLB2_{Tau}$ mice in both spatial learning and sucrose preference paradigms may indicate motor dysfunction, hence, 14-month old mice were evaluated in the balance beam paradigm. No impairment in performance was detected for any beam diameter or shape (Fig. 8 A+B). In fact, $PLB2_{Tau}$ mice performed somewhat better as indicated by lower traverse latencies in the least challenging diameter of the square beam test (interaction: $F_{(2,46)}$=6.142: p<0.01, post-hoc analysis p<0.01 for 28 cm diameter).

b) Circadian Activity and Exploratory Locomotion

Investigations of ambulatory activity of 6-month old $PLB2_{Tau}$ mice had demonstrated overall reduced activity, notable in each parameter studied. In the PhenoTyper, $PLB2_{Tau}$ mice demonstrated lower exploratory activity during the habituation phase compared with age matched PLB_{WT} mice ($F_{(1,340)}$=5.39, p<0.05, Fig. 9.A). A one phase decay non-linear fit of habituation data (considering Y0, plateau and K) indicated that the activity curves over the 180 min period were significantly different between genotypes (p<0.001), with faster kinetics in the transgenic group. However, considered individually there were no differences in the initial activity (Y0), the final baseline activity following habituation (plateau) or the rate at which activity declined (K).

Following the habituation phase, evidence for reduced exploratory activity persisted over time (genotype: $F_{(1,2093)}$=16.64, p<0.001, Fig. 9.B) as well as for the mean activity per hour over a 24 hr cycle ($F_{(1,552)}$=16.2, p<0.001, Fig. 9.C), the activity of $PLB2_{Tau}$ mice being particularly diminished during the initial hours of the dark phase. However overall a significant effect of genotype was observed for pooled mean light and dark phase activity ($F_{(1,25)}$=12.89, p<0.01, Fig. 9.D) and post-hoc analysis indicated decreased activity during both phases in $PLB2_{Tau}$ mice (light and dark, p<0.01).

c) Vigilance states and EEG recordings

The preceding data suggested a reduction in activity independent of day/night phase. However, quantification of EEG-guided vigilance stages during PhenoTyper recordings in 6-month old cohorts demonstrated that transgenic mice were in fact more awake, and significantly so during the light (rest) phase, despite the reduced motor activity. A selective disruption of sleep stages was confirmed only during the light (rest) phase (vigilance composition: state: $F_{(27,2)}$=1534, p<0.001 and interaction: $F_{(2,27)}$=47.02, p<0.001), when

$PLB2_{Tau}$ mice spent an increased time awake (Fig. 10.A, $p<0.001$) and correspondingly a decreased time in NREM ($p<0.001$). Nocturnal vigilance states were unaffected (Fig 10.A).

Spectral analysis of EEG recording from both hippocampal and prefrontal regions demonstrated overall significant interactions for both spectra during wakefulness ($F>1$, df= 380, $p<0.05$), largely due to a loss in alpha power in both frontal and parietal locations. During sleep, however, region- and stage-specific changes were also detected: REM spectra were overall affected only in the parietal channel, while NREM spectra differed only in the prefrontal location (effects of genotype and interaction for both: $p<0.001$). The most apparent change in the REM spectrum was an increase in delta power, while the prefrontal NREM spectrum was globally affected (see Fig. 10.B for full statistical band analysis).

d) Hippocampal Electrophysiology

Given the rather modest impairments of $PLB2_{Tau}$ in hippocampus-dependent tasks yet altered parietal EEG profiles, hippocampal slice electrophysiology was investigated for further evidence of intact vs. impaired hippocampal signalling. Initial input/output (I/O) curves generated for stimulation input vs. fEPSP slope indicated that basic hippocampal synaptic transmission was unaltered in $PLB2_{Tau}$ slices compared with PLB_{WT} slices at 6 and 12-months of age (Fig. 11.Ai + Aii, $p>0.05$ for both). However, an overall reduction in the evoked fEPSP slope across the stimulation range was observed at 24 months of age (Fig. 11.Aiii, genotype: $F_{(1,1104)}=28$, $p<0.001$). Evoked fEPSP slopes were also plotted against fibre volley amplitudes, indexing the degree of pre-synaptic depolarisation required to evoke postsynaptic depolarisation (Koss et al., 2013). Here, I/O curves demonstrated reduced presynaptic efficiency in eliciting postsynaptic depolarisation at all ages in $PLB2_{Tau}$ preparations compared to WT counterparts (Fig. 11.B: 6-months: $F_{(1,280)}=6.072$, $p<0.05$, 12-months: $F_{(1,240)}=7.169$, $p<0.001$ and 24-months of age: $F_{(1,340)}=29.53$, $p<0.001$). An age−dependent decline in pre- / post- synaptic efficiency was present in both PLB_{WT} and $PLB2_{Tau}$ mice (age effect: WT: $F_{(2,440)}=14.87$, $p<0.001$ and $PLB2_{Tau}$: $F_{(2,420)}=23.09$, $p<0.001$). Paired analysis between age groups indicated that the most pronounced deficit occurred from 12 to 24 months of age ($p<0.001$).

LTP was not significantly affected in $PLB2_{Tau}$ hippocampal slices at any age tested, despite reduced synaptic efficiency. However, at 12 months a strong trend for impaired LTP in $PLB2_{Tau}$ mice was observed (Fig. 11.C, $F_{(1,2242)}=3.394$, $p=0.07$). Further protocols for LTD and paired-pulse facilitation/ inhibition did not yield any alterations between WT and $PLB2_{Tau}$ mice (data not shown).

Discussion

We here report on a novel low-expression hTau knock-in model of FTD, the $PLB2_{Tau}$ mouse, which recapitulates key aspects of FTD. Phenotypically, $PLB2_{Tau}$ mice demonstrated disturbances in emotionality and pronounced semantic memory deficits alongside altered activity and vigilance yet only modest spatial learning deficits. Corresponding impairments in neuronal physiology revealed shifts in EEG power spectra and hippocampal transmission efficiency, while hippocampal synaptic plasticity was largely preserved. Functional disruptions emerged alongside increased tau phosphorylation without overt tau aggregation.

Emotional Phenotypes of $PLB2_{Tau}$ mice

The most striking changes observed in $PLB2_{Tau}$ mice relate to non-cognitive behavioural abnormalities evident in a number of emotional and motivation measures. Emotional disturbances in FTD patients comprise aberrant social behaviour, anxiety, apathy and disinhibition (Zamboni et al., 2008; Perri et al., 2014), which may correlate with prefrontal vs. temporal atrophy. $PLB2_{Tau}$ mice demonstrated heightened anxiety indicated not only by their behaviour within the EPM, but evident throughout all behavioural tests, such as decreased exploratory behaviour in the PhenoTyper, reduced corner visits in the IntelliCage and elevated swim speeds in the WM. This is in contrast to the unaffected anxiety levels or indeed the bold non-anxious behaviour described in many other FTD models (see Table 1). Such data have been interpreted as disinhibition, also frequently reported in FTD cases (Tanemura et al., 2002, Takeuchi et al., 2011). Here, the $PLB2_{Tau}$ mice demonstrated both elevated anxiety and traits of apathy and/or depression (anhedonia and reduced consumption of food and liquid provisions). Several clinical studies have indicated a high prevalence of anxiety in human FTD, (~50%, Porter et al., 2003, Chiu et al., 2006; Tartaglia et al., 2014), and stratification of the disease suggests comorbid depression in those FTD cases where anxiety is prominent (Mourik et al., 2004). Ultimately, it is difficult in mice to dissociate a depressive phenotype from one of apathy, frequently encountered early in FTD (>80%; Malloy et al., 2007; Rascovsky et al., 2011). In any case, emotional behaviour is often insufficiently determined in transgenic mice, but it is interesting to note that human symptoms correspond well to the apathetic (under undisturbed conditions) yet anxious (under stressful conditions) behaviour of $PLB2_{Tau}$ mice. The few studies which investigated the emotional phenotypes of FTD tau models describe decreased reward-seeking behaviour and increased forced swim test immobility, which

correlated with a diminished basal serotonergic tone within the frontal cortex (Egashira et al., 2005; Van der Jeugd et al., 2013).

Potentially as a result of altered emotionality, $PLB2_{Tau}$ mice demonstrated a robust hypoactive trait in many experimental parameters, most evident when monitoring circadian and ambient activity within the PhenoTyper. In this respect $PLB2_{Tau}$ mice present a similar global reduction in activity as observed in human FTD (Harper et al., 2001; Anderson et al., 2009). Hypoactivity and inertia being most pronounced during the initial waking hours, which was also observed here in $PLB2_{Tau}$ mice. Hypoactivity was present without any overt motor deficits, which are often confounding factors in many models with high tau expression (see Table 1). Even in models employing forebrain specific promoters (Santacruz et al., 2005), a loss of cortico-spinal neurons coincided with the progressive emergence of motor deficits, yet here as well as in other low expression models (Tatebayashi et al., 2002) such impairments could be avoided. Instead, the reduced exploratory activity in addition to the more rapid habituation may index a state of apathy or anxiety (Salomons et al., 2010). Furthermore, increased wakefulness and a reduction in NREM sleep of the $PLB2_{Tau}$ mice rule out increased sleep time as the reason for reduced exploratory activity. In this respect, $PLB2_{Tau}$ mice present a highly FTD relevant phenotype as sleep disturbances are common in all dementias (Guarnieri et al., 2012), with reduced sleep duration commonly reported in FTD cases (Bombois et al., 2010; Bonakis et al., 2014).

Distinct cognitive deficits of $PLB2_{Tau}$ mice

Though behavioural and emotional disruptions typify FTD symptomatology, cognitive deficits are also key symptoms. Well established are semantic memory problems, which present during the early manifestations of FTD, particular in those cases diagnosed as svFTD (Rogers et al., 2006; Rascovsky et al., 2007). Corresponding impairments were evident in the $PLB2_{Tau}$ mice at 6 months of age in the STFP paradigm. This task depends on several behavioural facets, such as sociability, olfaction and semantic memory, with neuroanatomical correlates in the pre-frontal and hippocampal regions (Van der Kooji and Sandi, 2012). Both sociability and olfaction of $PLB2_{Tau}$ mice were unaltered, yet a preference for cued food was not established independent of the delay.

The deficit in semantic memory was in contrast to intact spatial learning demonstrated in the MW of both 6- and 12-months old $PLB2_{Tau}$ mice. Though many previous FTD mouse models (including the rTg4510 model which also utilises the forebrain specific CaMKIIα promoter) report spatial deficits in acquisition as well as recall (see Table 1), the intact WM performance observed here is again in keeping with other models where tau expression is low (Tanemura et al., 2002). The absence of robust dysfunction in non-overexpressing models is suggestive of a dose-dependent relationship between tau and hippocampal impairment. Here, when spatial memory was further assessed in the corner learning

paradigm of the IntelliCage, 6-month old $PLB2_{Tau}$ mice presented with only modest impairments which marginally progressed in severity with age. The discrepancy in performance between the two paradigms may indicate an influence of test parameters on performance: The WM utilises repeated temporal exposure to an adverse and stressful situation, whilst the IntelliCage exploits innate explorative behaviour and the urge for water intake. Together, the impaired learning in the corner learning task suggests reduced motivation and exploration (as discussed above), amidst modest hippocampal dysfunction. Deficits during IntelliCage testing were however apparent in the reversal learning paradigm. The poor performance of $PLB2_{Tau}$ mice may indicate a mild deficit in hippocampal function alongside a more prominent dysfunction in prefrontal cortical processing, given this region's involvement in reversal learning (de Bruin et al 1994; Lacroix et al., 2002; Murray et al., 2015) and may be relevant for the executive dysfunction and stereotyped mental rigidity observed in FTD patients (Bozeat et al., 2000; Stopford et al., 2012).

In humans, spatial memory is also commonly preserved in the early stages of FTD, while motivational and attentional deficits are often encountered, which reportedly introduce confounding factors for various memory tasks (Stopford et al., 2012). Indeed, this profile of selective deficits may provide further evidence of the FTD relevant phenotype of the $PLB2_{Tau}$ mice, expressing prominent semantic deficits earlier than spatial memory deficits, potentially reflecting a vulnerability of higher neuronal processes (semantic vs. spatial learning) and regions (prefrontal vs. temporal) relevant to FTD tau pathology. Similar findings have been reported in the THY-Tau22 mouse model, where non-spatial memory was affected prior to spatial memory, although only a modest reduction in STFP was observed (Van der Jeugd et al., 2013) and are in agreement with results in L66 (Melis et al., 2015) and V337M models (Tamemura et al., 2001).

Interestingly, we have previously reported deficits in WM acquisition at 12 months and corner learning at 4 months in the related $PLB1_{Triple}$ mouse which expresses the same hTau transgene alongside mutant hAPP and PS1 (Platt et al., 2011; Ryan et al., 2013), suggesting that the IntelliCage may be more sensitive than the WM to detect spatial learning impairments. Alternatively as $PLB1_{Triple}$ mice serve as a model of AD, where spatial learning impairments are early and defining symptoms of the disease, the divergent cognitive phenotypes of $PLB2_{Tau}$ and $PLB1_{Triple}$ mice may highlight differential behavioural traits induced by a combination of AD and FTD-Tau familial mutations when compared to FTD-Tau mutants alone.

Electrophysiological phenotypes of $PLB2_{Tau}$ mice

Region-specific physiological changes that may underpin parietal (hippocampal) vs. frontal changes were uncovered in *in vivo* EEG recordings, while hippocampal slice experiments confirmed a mild impairment in synaptic transmission only. The most striking changes in

EEG spectra were a reduction in alpha power for both brain regions in awake $PLB2_{Tau}$ mice, and an increase in delta power during REM sleep specific to the parietal channel. This agreed by and large with the phenotype encountered in $PLB1_{Triple}$ mice (Platt et al., 2011). However, sleep spectra of $PLB2_{Tau}$ mice showed a much clearer region- and stage-specific profile and overall more robust spectral changes, contrasting with subtle and band-specific EEG changes of the triple transgenic mice at this age.

Of the limited work conducted on EEG in FTD patients and FTD models, early observations suggest that EEG abnormalities are milder compared with AD, and standard EEG parameters may appear normal in FTD amidst altered behaviour and cognition (see Micanovic and Pal, 2014 for review). However, the recent adoption of quantitative EEG (qEEG) measures has demonstrated reduced power particularly in alpha and beta bands in FTD patients (Lindau et al., 2003). Clearly, further studies are required, as this approach may provide valuable translational and diagnostic value (Platt & Riedel, 2011; Platt, Welch & Riedel, 2011). In particular, novel qEEG parameters and network analyses may offer improved disease-specific criteria (Farb et al., 2013; Wessel et al., 2015).

A correlate of changes in hippocampal power spectra may be found within altered synaptic efficiency observed in hippocampal slices from $PLB2_{Tau}$ mice. Here, a reduction in basal synaptic transmission emerged early (at 6 months), with only a modest impact on LTP at 12 months. Intact LTP agrees with sustained WM performance (Whitlock et al., 2006; Nabavi et al., 2014), and with the proposition that altered motivation and impaired prefrontal processing may have contributed to deficits in other cognitive tasks. Corresponding investigations in other transgenic Tau models has yielded diverse and somewhat contradictory results, e.g. decreased basal synaptic efficiency in the absence of altered LTP (Schindowski et al., 2006), or in combination with impaired LTP (Yoshiyama et al., 2007) or impaired LTP only (Rosenmann et al., 2008, Hoover et al., 2010; Van der Jeugd et al., 2012). These inconsistencies are likely due to the varying level of transgene expression and electrophysiological protocols. Impairments in synaptic physiology may also be dependent on the specific FTD tau mutations and the resultant degenerative mechanism (Lee et al., 2009, Tackenberg and Brandt, 2009). Intriguingly, a reduction in basal synaptic efficacy was only observed $\geq$12 months in the related $PLB1_{Triple}$ mouse model of AD (Koss et al., 2013) while LTP was affected from 6 months onwards, despite the expression of the identical tau transgene, again suggestive of transgene-specific yet non-additive degenerative mechanisms.

Transgene Expression and Protein Profiles

In comparison with many previous hTau models, $PLB2_{Tau}$ mice express low levels of the transgene, originating from the single *hTau* vector knock-in and a region-specific regulatory element. This low level was sufficient to induce highly FTD relevant phenotypes. The subtle increase in a specific 60 kDa Tau species reported here must be considered crucial as the

majority of existing hTau models show overexpression (up to 13 fold of total endogenous Tau, see Table 1). Though pronuclear injection derived models can provide robust phenotypes with a short pre-symptomatic period, the $PLB2_{Tau}$ model may limit any potential confounding pathology derived from Tau overexpression, which could mask mechanistic differences between FTD mutant driven Tau dysfunction and those reported in animal models from the overexpression of non-mutant hTau (Spittaels et al., 1999; Polydoro et al., 2009).

The single hTau species migrating at 60 kDa (corresponding to the 2N4R isoform, Buee et al., 2000) detected here was present alongside an additional elevation of Tau protein at 55 kDa, indicative of a modest increase in endogenous murine Tau, in agreement with other models where endogenous Tau was subject to accumulation, hyper-phosphorylation and aggregation (Mocanu et al., 2008, Cowan et al., 2010; Baglietto-Vargas et al., 2014). Abnormal elevations in tau phosphorylation at the PHF-1, CP-13 and AT-8 epitopes initially affected endogenous murine Tau, most prominently at the major 50 kDa species, but by 12 months of age progressed to encompass all remaining isoforms. Despite the elevation in tau phosphorylation there was no notable shift in electrophoretic migration nor the emergence of specific hyperphosphorylated species as reported in human AD cases (Flament and Delacourte, 1989) and in several FTD Tau mouse models (Berger et al., 2007; Sahara et al., 2013). The evidence present here suggests that elevations in tau phosphorylation may be sufficient to driving quantifiable behavioural phenotypes.

Both P301L and R406W mutations contained within the hTau transgene could contribute to the pathogenic mechanism underlying the observed phenotypes. R406W containing Tau, alone or in combination with other FTD mutations, has previously been reported to lower Tau phosphorylation at some epitopes in both cellular (Gauthier-Kemper et al. 2011) and animal models (Lim et al., 2001; Zhang et al., 2004). Such an anomaly is particularly evident at the PHF-1 epitope (Ser396/Ser404), as the missense mutation restricts GSK-3β kinase accesses (Vogelsberg-Ragaglia et al., 2000). However, in human FTD R406W cases, the phosphorylation of the PHF-1 epitope is enhanced, predominantly due to phosphorylation of non-mutated Tau in the soluble fraction (Miyasaka et al., 2001). Correspondingly, the increase in PHF-1 positive Tau in $PLB2_{Tau}$ mice may reflect the progressive phosphorylation primarily of the endogenous murine Tau species.

The emergence of phospho-tau pathology in the $PLB2_{Tau}$ mouse is an important demonstration of tau phospho-pathology without overt overexpression. It is at present unclear why the previously generated P301L KI Tau mouse failed to demonstrate cognitive deficits and presented with Tau hypo-phosphorylation (Gilley et al., 2012). Increased Tau hyperphosphorylation had been consistently reported in conventional P301L models (Lewis et al., 2000, Gotz et al., 2001, Santa Cruz et al., 2005; Terwel et al., 2005), hence overexpression could be assumed to be a causative factor for such phosphorylation (see

Table 1). However, our data argue against this and may suggest that the problem of the P301L KI model lies within the substitution of proline with lysine at amino acid residue 290, which may not be comparable with the substitution at residue 301 of the human tau gene. As both PHF-1 and AT-8 are regarded to detect late stage phospho-epitopes associated with NFTs (Augustinack et al., 2002), it is perhaps surprising that no phospho- or total Tau was detected within the insoluble fraction of our preparations. However, AT-8 and PHF-1 immunoreactivity is not exclusively associated with NFTs, as AT-8 positive neuropil threads and pre-tangle neurons were detected in human AD cases (Lasagna-Reeves et al., 2012) and each epitope is readily detected in soluble tau extracts from tauopathies and animal models (see Anderson et al., 2008 and Deter et al., 2008 for examples). Together, our data strongly suggest that $PLB2_{Tau}$ mice present with elevated levels of soluble phospho-Tau species without the overt presence of insoluble aggregates within the age-range investigated. A progressive deposition of Tau may indeed occur later, but the onset of behavioural abnormalities correlated with the emergence of elevated soluble Tau phosphorylation, in agreement with observations in other Tau models (Berger et al., 2007; Flunkert et al., 2013; Koss et al., 2015) and is supportive of the disruption of neuronal function associated with soluble tau pathology rather than the presence of aggregated tau species (Fox et al., 2011; Polyodoro et al., 2014). The implicated toxicity of soluble phospho-tau is further in keeping with the lack of behavioural deficits detected within the life-span of P301L KI mice where tau is hypo-phosphorylated (Gilley et al., 2012).

Conclusions

$PLB2_{Tau}$ mice express low hTau transgene levels specifically in the forebrain, which yields subtle hTau protein expression and phospho-tau pathology that incorporates both murine and transgenic tau species. This drives highly FTD relevant phenotypes related to semantic memory, anxiety, anhedonia, sleep and activity, with only mild age-dependent impairments in spatial learning. The selective development of electrophysiological, behavioural and cognitive changes in $PLB2_{Tau}$ mice highlight the specific vulnerability of neuronal networks to tau pathology and associated disruptions in neuronal communication. In particular, the emergence of semantic memory deficit together with FTD-relevant emotional disturbances amidst largely preserved spatial memory suggests that $PLB2_{Tau}$ mice can serve as a highly relevant model of FTD rather than AD, with a strong translational potential.

References

ALLEN, B., INGRAM, E., TAKAO, M., SMITH, M.J., JAKES, R., VIRDEE, K., YOSHIDA, H., HOLZER, M., CRAXTON, M., EMSON, P.C., ATZORI, C., MIGHELI, A., CROWTHER, R.A., GHETTI, B., SPILLANTINI, M.G. and GOEDERT, M., 2002. Abundant tau filaments and nonapoptotic neurodegeneration in transgenic mice expressing human P301S tau protein. The Journal of Neuroscience, 22(21), pp. 9340-9351.

ANDERSON, J.M., HAMPTON, D.W., PATANI, R., PRYCE, G., CROWTHER, R.A., REYNOLDS, R., FRANKLIN, R.J., GIOVANNONI, G., COMPSTON, D.A., BAKER, D., SPILLANTINI, M.G. and CHANDRAN, S., 2008. Abnormally phosphorylated tau is associated with neuronal and axonal loss in experimental autoimmune encephalomyelitis and multiple sclerosis. Brain, 131(Pt 7), pp. 1736-1748.

ANDERSON, K.N., HATFIELD, C., KIPPS, C., HASTINGS, M. and HODGES, J.R., 2009. Disrupted sleep and circadian patterns in frontotemporal dementia. European Journal of Neurology, 16(3), pp. 317-323.

AUGUSTINACK, J.C., SCHNEIDER, A., MANDELKOW, E.M. and HYMAN, B.T., 2002. Specific tau phosphorylation sites correlate with severity of neuronal cytopathology in Alzheimer's disease. Acta Neuropathologica, **103**(1), pp. 26-35.

BAGLIETTO-VARGAS, D., KITAZAWA, M., LE, E.J., ESTRADA-HERNANDEZ, T., RODRIGUEZ-ORTIZ, C.J., MEDEIROS, R., GREEN, K.N. and LAFERLA, F.M., 2014. Endogenous murine tau promotes neurofibrillary tangles in 3xTg-AD mice without affecting cognition. Neurobiology of Disease, 62, pp. 407-415.

BAILEY, R.M., HOWARD, J., KNIGHT, J., SAHARA, N., DICKSON, D.W. and LEWIS, J., 2014. Effects of the C57BL/6 strain background on tauopathy progression in the rTg4510 mouse model. Molecular Neurodegeneration, 9, pp. 8-1326-9-8.

BERGER, Z., RODER, H., HANNA, A., CARLSON, A., RANGACHARI, V., YUE, M., WSZOLEK, Z., ASHE, K., KNIGHT, J., DICKSON, D., ANDORFER, C., ROSENBERRY, T.L., LEWIS, J., HUTTON, M. and JANUS, C., 2007. Accumulation of pathological tau species and memory loss in a conditional model of tauopathy. The Journal of Neuroscience, 27(14), pp. 3650-3662.

BOMBOIS, S., DERAMBURE, P., PASQUIER, F. and MONACA, C., 2010. Sleep disorders in aging and dementia. The Journal of Nutrition, Health & Aging, 14(3), pp. 212-217.

BONAKIS, A., ECONOMOU, N.T., PAPARRIGOPOULOS, T., BONANNI, E., MAESTRI, M., CARNICELLI, L., DI COSCIO, E., KTONAS, P., VAGIAKIS, E., THEODOROPOULOS, P. and PAPAGEORGIOU, S.G., 2014. Sleep in frontotemporal dementia is equally or possibly more disrupted, and at an earlier stage, when compared to sleep in Alzheimer's disease. Journal of Alzheimer's Disease, 38(1), pp. 85-91.

BOZEAT, S., GREGORY, C.A., RALPH, M.A. and HODGES, J.R., 2000. Which neuropsychiatric and behavioural features distinguish frontal and temporal variants of frontotemporal dementia from Alzheimer's disease? Journal of Neurology, Neurosurgery, and Psychiatry, 69(2), pp. 178-186.

BROOKS, S.P., PASK, T., JONES, L. and DUNNETT, S.B., 2005. Behavioural profiles of inbred mouse strains used as transgenic backgrounds. II: cognitive tests. Genes, Brain, and Behavior, 4(5), pp. 307-317.

BUEE, L., BUSSIERE, T., BUEE-SCHERRER, V., DELACOURTE, A. and HOF, P.R., 2000. Tau protein isoforms, phosphorylation and role in neurodegenerative disorders. Brain Research Reviews, 33(1), pp. 95-130.

CALAMAI, E., DALL'ANGELO, S., KOSS, D., DOMARKAS, J., MCCARTHY, T.J., MINGARELLI, M., RIEDEL, G., SCHWEIGER, L.F., WELCH, A., PLATT, B. and ZANDA, M., 2013. 18F-barbiturates are PET tracers with diagnostic potential in Alzheimer's disease. Chemical Communications, 49(8), pp. 792-794.

CHIU, M.J., CHEN, T.F., YIP, P.K., HUA, M.S. and TANG, L.Y., 2006. Behavioral and psychologic symptoms in different types of dementia. Journal of the Formosan Medical Association, 105(7), pp. 556-562.

COWAN, C.M., BOSSING, T., PAGE, A., SHEPHERD, D. and MUDHER, A., 2010. Soluble hyper-phosphorylated tau causes microtubule breakdown and functionally compromises normal tau in vivo. Acta Neuropathologica, 120(5), pp. 593-604.

CROWTHER, R.A., 1991. Straight and paired helical filaments in Alzheimer disease have a common structural unit. Proceedings of the National Academy of Sciences of the United States of America, 88(6), pp. 2288-2292.

DE BRUIN, J.P., SANCHEZ-SANTED, F., HEINSBROEK, R.P., DONKER, A. and POSTMES, P., 1994. A behavioural analysis of rats with damage to the medial prefrontal cortex using the Morris water maze: evidence for behavioural flexibility, but not for impaired spatial navigation. Brain Research, 652(2), pp. 323-333.

DE CALIGNON, A., POLYDORO, M., SUAREZ-CALVET, M., WILLIAM, C., ADAMOWICZ, D.H., KOPEIKINA, K.J., PITSTICK, R., SAHARA, N., ASHE, K.H., CARLSON, G.A., SPIRES-JONES, T.L. and HYMAN, B.T., 2012. Propagation of tau pathology in a model of early Alzheimer's disease. Neuron, 73(4), pp. 685-697.

DETERS, N., ITTNER, L.M. and GOTZ, J., 2008. Divergent phosphorylation pattern of tau in P301L tau transgenic mice. The European Journal of Neuroscience, 28(1), pp. 137-147.

EGASHIRA, N., IWASAKI, K., TAKASHIMA, A., WATANABE, T., KAWABE, H., MATSUDA, T., MISHIMA, K., CHIDORI, S., NISHIMURA, R. and FUJIWARA, M., 2005. Altered depression-related behavior and neurochemical changes in serotonergic neurons in mutant R406W human tau transgenic mice. Brain Research, 1059(1), pp. 7-12.

FARB, N.A., GRADY, C.L., STROTHER, S., TANG-WAI, D.F., MASELLIS, M., BLACK, S., FREEDMAN, M., POLLOCK, B.G., CAMPBELL, K.L., HASHER, L. and CHOW, T.W., 2013. Abnormal network connectivity in frontotemporal dementia: evidence for prefrontal isolation. Cortex, 49(7), pp. 1856-1873.

FLAMENT, S. and DELACOURTE, A., 1989. Abnormal tau species are produced during Alzheimer's disease neurodegenerating process. FEBS letters, 247(2), pp. 213-216.

FLUNKERT, S., HIERZER, M., LOFFLER, T., RABL, R., NEDDENS, J., DULLER, S., SCHOFIELD, E.L., WARD, M.A., POSCH, M., JUNGWIRTH, H., WINDISCH, M. and HUTTER-PAIER, B., 2013. Elevated levels of soluble total and hyperphosphorylated tau result in early behavioral deficits and distinct changes in brain pathology in a new tau transgenic mouse model. Neuro-degenerative Diseases, 11(4), pp. 194-205.

FOX, L.M., WILLIAM, C.M., ADAMOWICZ, D.H., PITSTICK, R., CARLSON, G.A., SPIRES-JONES, T.L. and HYMAN, B.T., 2011. Soluble tau species, not neurofibrillary aggregates, disrupt neural system integration in a tau transgenic model. Journal of Neuropathology and Experimental Neurology, 70(7), pp. 588-595.

FURUKAWA, K., WANG, Y., YAO, P.J., FU, W., MATTSON, M.P., ITOYAMA, Y., ONODERA, H., D'SOUZA, I., POORKAJ, P.H., BIRD, T.D. and SCHELLENBERG, G.D., 2003. Alteration in calcium channel properties is responsible for the neurotoxic action of a familial frontotemporal dementia tau mutation. Journal of Neurochemistry, 87(2), pp. 427-436.

GAMA SOSA, M.A., DE GASPERI, R. and ELDER, G.A., 2010. Animal transgenesis: an overview. Brain Structure & Function, 214(2-3), pp. 91-109.

GAUTHIER-KEMPER, A., WEISSMANN, C., GOLOVYASHKINA, N., SEBO-LEMKE, Z., DREWES, G., GERKE, V., HEINISCH, J.J. and BRANDT, R., 2011. The frontotemporal dementia mutation R406W blocks tau's interaction with the membrane in an annexin A2-dependent manner. The Journal of Cell Biology, 192(4), pp. 647-661.

GHOSH, S. and LIPPA, C.F., 2015. Clinical Subtypes of Frontotemporal Dementia. American Journal of Alzheimer's Disease and Other Dementias, 30(7), pp. 653-661.

GILLEY, J., SEEREERAM, A., ANDO, K., MOSELY, S., ANDREWS, S., KERSCHENSTEINER, M., MISGELD, T., BRION, J.P., ANDERTON, B., HANGER, D.P. and COLEMAN, M.P., 2012. Age-dependent axonal transport and locomotor changes and tau hypophosphorylation in a "P301L" tau knockin mouse. Neurobiology of Aging, 33(3), pp. 621.e1-621.e15.

GOEDERT, M., WISCHIK, C.M., CROWTHER, R.A., WALKER, J.E. and KLUG, A., 1988. Cloning and sequencing of the cDNA encoding a core protein of the paired helical filament of Alzheimer disease: identification as the microtubule-associated protein tau. Proceedings of the National Academy of Sciences of the United States of America, 85(11), pp. 4051-4055.

GOEDERT, M. and SPILLANTINI, M.G., 2000. Tau mutations in frontotemporal dementia FTDP-17 and their relevance for Alzheimer's disease. Biochimica et Biophysica Acta, 1502(1), pp. 110-121.

GOEDERT, M., GHETTI, B. and SPILLANTINI, M.G., 2012. Frontotemporal dementia: implications for understanding Alzheimer disease. Cold Spring Harbor Perspectives in Medicine, 2(2), pp. a006254.

GOTZ, J., CHEN, F., BARMETTLER, R. and NITSCH, R.M., 2001. Tau filament formation in transgenic mice expressing P301L tau. The Journal of Biological Chemistry, 276(1), pp. 529-534.

GUARNIERI, B., ADORNI, F., MUSICCO, M., APPOLLONIO, I., BONANNI, E., CAFFARRA, P., CALTAGIRONE, C., CERRONI, G., CONCARI, L., COSENTINO, F.I., FERRARA, S., FERMI, S., FERRI, R., GELOSA, G., LOMBARDI, G., MAZZEI, D., MEARELLI, S., MORRONE, E., MURRI, L., NOBILI, F.M., PASSERO, S., PERRI, R., ROCCHI, R., SUCAPANE, P., TOGNONI, G., ZABBERONI, S. and SORBI, S., 2012. Prevalence of sleep disturbances in mild cognitive impairment and dementing disorders: a multicenter Italian clinical cross-sectional study on 431 patients. Dementia and Geriatric Cognitive Disorders, 33(1), pp. 50-58.

HARPER, D.G., STOPA, E.G., MCKEE, A.C., SATLIN, A., HARLAN, P.C., GOLDSTEIN, R. and VOLICER, L., 2001. Differential circadian rhythm disturbances in men with Alzheimer disease and frontotemporal degeneration. Archives of General Psychiatry, 58(4), pp. 353-360.

HOOVER, B.R., REED, M.N., SU, J., PENROD, R.D., KOTILINEK, L.A., GRANT, M.K., PITSTICK, R., CARLSON, G.A., LANIER, L.M., YUAN, L.L., ASHE, K.H. and LIAO, D., 2010. Tau mislocalization to dendritic spines mediates synaptic dysfunction independently of neurodegeneration. Neuron, 68(6), pp. 1067-1081.

HRNKOVA, M., ZILKA, N., MINICHOVA, Z., KOSON, P. and NOVAK, M., 2007. Neurodegeneration caused by expression of human truncated tau leads to progressive neurobehavioural impairment in transgenic rats. Brain Research, 1130(1), pp. 206-213.

HUNSBERGER, H.C., RUDY, C.C., WEITZNER, D.S., ZHANG, C., TOSTO, D.E., KNOWLAN, K., XU, Y. and REED, M.N., 2014. Effect size of memory deficits in mice with adult-onset P301L tau expression. Behavioural Brain Research, 272, pp. 181-195.

HUTCHINSON, A.D. and MATHIAS, J.L., 2007. Neuropsychological deficits in frontotemporal dementia and Alzheimer's disease: a meta-analytic review. Journal of Neurology, Neurosurgery, and Psychiatry, 78(9), pp. 917-928.

JYOTI, A., PLANO, A., RIEDEL, G. and PLATT, B., 2015. Progressive age-related changes in sleep and EEG profiles in the PLB1Triple mouse model of Alzheimer's disease. Neurobiology of Aging, 36(10), pp. 2768-2784.

KHANDELWAL, P.J., DUMANIS, S.B., HERMAN, A.M., REBECK, G.W. and MOUSSA, C.E., 2012. Wild type and P301L mutant Tau promote neuro-inflammation and alpha-Synuclein accumulation in lentiviral gene delivery models. Molecular and Cellular Neurosciences, 49(1), pp. 44-53.

KOPPEL, J., JIMENEZ, H., AZOSE, M., D'ABRAMO, C., ACKER, C., BUTHORN, J., GREENWALD, B.S., LEWIS, J., LESSER, M., LIU, Z. and DAVIES, P., 2014. Pathogenic tau species drive a psychosis-like phenotype in a mouse model of Alzheimer's disease. Behavioural Brain Research, 275, pp. 27-33.

KOSS, D.J., DREVER, B.D., STOPPELKAMP, S., RIEDEL, G. and PLATT, B., 2013. Age-dependent changes in hippocampal synaptic transmission and plasticity in the PLB1Triple Alzheimer mouse. Cellular and Molecular Life Sciences, 70(14), pp. 2585-2601.

KOSS, D.J., ROBINSON, L., MIETELSKA-POROWSKA, A., GASIOROWSKA, A., SEPCIC, K., TURK, T., JASPARS, M., NIEWIADOMSKA, G., SCOTT, R.H., PLATT, B. and RIEDEL, G., 2015. Polymeric alkylpyridinium salts permit intracellular delivery of human Tau in rat hippocampal neurons: requirement of Tau phosphorylation for functional deficits. Cellular and Molecular Life Sciences, 72(23), pp. 4613-4632.

LACROIX, L., WHITE, I. and FELDON, J., 2002. Effect of excitotoxic lesions of rat medial prefrontal cortex on spatial memory. Behavioural Brain Research, 133(1), pp. 69-81.

LASAGNA-REEVES, C.A., CASTILLO-CARRANZA, D.L., SENGUPTA, U., SARMIENTO, J., TRONCOSO, J., JACKSON, G.R. and KAYED, R., 2012. Identification of oligomers at early stages of tau aggregation in Alzheimer's disease. FASEB Journal, 26(5), pp. 1946-1959.

LEE, S., JUNG, C., LEE, G. and HALL, G.F., 2009. Exonic point mutations of human tau enhance its toxicity and cause characteristic changes in neuronal morphology, tau distribution and tau phosphorylation in the lamprey cellular model of tauopathy. Journal of Alzheimer's Disease, 16(1), pp. 99-111.

LEWIS, J., MCGOWAN, E., ROCKWOOD, J., MELROSE, H., NACHARAJU, P., VAN SLEGTENHORST, M., GWINN-HARDY, K., PAUL MURPHY, M., BAKER, M., YU, X., DUFF, K., HARDY, J., CORRAL, A., LIN, W.L., YEN, S.H., DICKSON, D.W., DAVIES, P. and HUTTON, M.,

2000. Neurofibrillary tangles, amyotrophy and progressive motor disturbance in mice expressing mutant (P301L) tau protein. Nature Genetics, 25(4), pp. 402-405.

LEWIS, J., DICKSON, D.W., LIN, W.L., CHISHOLM, L., CORRAL, A., JONES, G., YEN, S.H., SAHARA, N., SKIPPER, L., YAGER, D., ECKMAN, C., HARDY, J., HUTTON, M. and MCGOWAN, E., 2001. Enhanced neurofibrillary degeneration in transgenic mice expressing mutant tau and APP. Science, 293(5534), pp. 1487-1491.

LIM, F., HERNANDEZ, F., LUCAS, J.J., GOMEZ-RAMOS, P., MORAN, M.A. and AVILA, J., 2001. FTDP-17 mutations in tau transgenic mice provoke lysosomal abnormalities and Tau filaments in forebrain. Molecular and Cellular Neurosciences, 18(6), pp. 702-714.

LINDAU, M., JELIC, V., JOHANSSON, S.E., ANDERSEN, C., WAHLUND, L.O. and ALMKVIST, O., 2003. Quantitative EEG abnormalities and cognitive dysfunctions in frontotemporal dementia and Alzheimer's disease. Dementia and Geriatric Cognitive Disorders, 15(2), pp. 106-114.

MALLOY, P., TREMONT, G., GRACE, J. and FRAKEY, L., 2007. The Frontal Systems Behavior Scale discriminates frontotemporal dementia from Alzheimer's disease. Alzheimer's & dementia : the journal of the Alzheimer's Association, 3(3), pp. 200-203.

MCMILLAN, P., KORVATSKA, E., POORKAJ, P., EVSTAFJEVA, Z., ROBINSON, L., GREENUP, L., LEVERENZ, J., SCHELLENBERG, G.D. and D'SOUZA, I., 2008. Tau isoform regulation is region- and cell-specific in mouse brain. The Journal of Comparative Neurology, 511(6), pp. 788-803.

MELIS, V., ZABKE, C., STAMER, K., MAGBAGBEOLU, M., SCHWAB, K., MARSCHALL, P., VEH, R.W., BACHMANN, S., DEIANA, S., MOREAU, P.H., DAVIDSON, K., HARRINGTON, K.A., RICKARD, J.E., HORSLEY, D., GARMAN, R., MAZURKIEWICZ, M., NIEWIADOMSKA, G., WISCHIK, C.M., HARRINGTON, C.R., RIEDEL, G. and THEURING, F., 2015. Different pathways of molecular pathophysiology underlie cognitive and motor tauopathy phenotypes in transgenic models for Alzheimer's disease and frontotemporal lobar degeneration. Cellular and Molecular Life Sciences, 72(11), pp. 2199-2222.

MENDEZ, M.F., SHAPIRA, J.S., WOODS, R.J., LICHT, E.A. and SAUL, R.E., 2008. Psychotic symptoms in frontotemporal dementia: prevalence and review. Dementia and Geriatric Cognitive Disorders, 25(3), pp. 206-211.

MICANOVIC, C. and PAL, S., 2014. The diagnostic utility of EEG in early-onset dementia: a systematic review of the literature with narrative analysis. Journal of Neural Transmission, 121(1), pp. 59-69.

MIYASAKA, T., MORISHIMA-KAWASHIMA, M., RAVID, R., HEUTINK, P., VAN SWIETEN, J.C., NAGASHIMA, K. and IHARA, Y., 2001. Molecular analysis of mutant and wild-type tau

deposited in the brain affected by the FTDP-17 R406W mutation. The American Journal of Pathology, 158(2), pp. 373-379.

MOCANU, M.M., NISSEN, A., ECKERMANN, K., KHLISTUNOVA, I., BIERNAT, J., DREXLER, D., PETROVA, O., SCHONIG, K., BUJARD, H., MANDELKOW, E., ZHOU, L., RUNE, G. and MANDELKOW, E.M., 2008. The potential for beta-structure in the repeat domain of tau protein determines aggregation, synaptic decay, neuronal loss, and coassembly with endogenous Tau in inducible mouse models of tauopathy. The Journal of Neuroscience, 28(3), pp. 737-748.

MOURIK, J.C., ROSSO, S.M., NIERMEIJER, M.F., DUIVENVOORDEN, H.J., VAN SWIETEN, J.C. and TIBBEN, A., 2004. Frontotemporal dementia: behavioral symptoms and caregiver distress. Dementia and Geriatric Cognitive Disorders, 18(3-4), pp. 299-306.

MURRAY, A.J., WOLOSZYNOWSKA-FRASER, M.U., ANSEL-BOLLEPALLI, L., COLE, K.L., FOGGETTI, A., CROUCH, B., RIEDEL, G. and WULFF, P., 2015. Parvalbumin-positive interneurons of the prefrontal cortex support working memory and cognitive flexibility. Scientific Reports, 5, pp. 16778.

NABAVI, S., FOX, R., PROULX, C.D., LIN, J.Y., TSIEN, R.Y. and MALINOW, R., 2014. Engineering a memory with LTD and LTP. Nature, 511(7509), pp. 348-352.

NEUMANN, M., TOLNAY, M. and MACKENZIE, I.R., 2009. The molecular basis of frontotemporal dementia. Expert Reviews in Molecular Medicine, 11, pp. e23.

ODDO, S., CACCAMO, A., SHEPHERD, J.D., MURPHY, M.P., GOLDE, T.E., KAYED, R., METHERATE, R., MATTSON, M.P., AKBARI, Y. and LAFERLA, F.M., 2003. Triple-transgenic model of Alzheimer's disease with plaques and tangles: intracellular Abeta and synaptic dysfunction. Neuron, 39(3), pp. 409-421.

PERRI, R., MONACO, M., FADDA, L., CALTAGIRONE, C. and CARLESIMO, G.A., 2014. Neuropsychological correlates of behavioral symptoms in Alzheimer's disease, frontal variant of frontotemporal, subcortical vascular, and lewy body dementias: a comparative study. Journal of Alzheimer's Disease, 39(3), pp. 669-677.

PETRY, F.R., PELLETIER, J., BRETTEVILLE, A., MORIN, F., CALON, F., HEBERT, S.S., WHITTINGTON, R.A. and PLANEL, E., 2014. Specificity of anti-tau antibodies when analyzing mice models of Alzheimer's disease: problems and solutions. PloS one, 9(5), pp. e94251.

PLATT, B., DREVER, B., KOSS, D., STOPPELKAMP, S., JYOTI, A., PLANO, A., UTAN, A., MERRICK, G., RYAN, D., MELIS, V., WAN, H., MINGARELLI, M., PORCU, E., SCROCCHI, L., WELCH, A. and RIEDEL, G., 2011. Abnormal cognition, sleep, EEG and brain metabolism in a novel knock-in Alzheimer mouse, PLB1. PloS one, 6(11), pp. e27068.

PLATT, B. and RIEDEL, G., 2011. The cholinergic system, EEG and sleep. Behavioural Brain Research, 221(2), pp. 499-504.

PLATT, B., WELCH, A. and RIEDEL, G., 2011. FDG-PET imaging, EEG and sleep phenotypes as translational biomarkers for research in Alzheimer's disease. Biochemical Society Transactions, 39(4), pp. 874-880.

PLUCINSKA, K., CROUCH, B., KOSS, D., ROBINSON, L., SIEBRECHT, M., RIEDEL, G. and PLATT, B., 2014. Knock-in of human BACE1 cleaves murine APP and reiterates Alzheimer-like phenotypes. The Journal of Neuroscience, 34(32), pp. 10710-10728.

PODHORNA, J. and BROWN, R.E., 2002. Strain differences in activity and emotionality do not account for differences in learning and memory performance between C57BL/6 and DBA/2 mice. Genes, Brain, and Behavior, 1(2), pp. 96-110.

POLYDORO, M., ACKER, C.M., DUFF, K., CASTILLO, P.E. and DAVIES, P., 2009. Age-dependent impairment of cognitive and synaptic function in the htau mouse model of tau pathology. The Journal of Neuroscience, 29(34), pp. 10741-10749.

POLYDORO, M., DZHALA, V.I., POOLER, A.M., NICHOLLS, S.B., MCKINNEY, A.P., SANCHEZ, L., PITSTICK, R., CARLSON, G.A., STALEY, K.J., SPIRES-JONES, T.L. and HYMAN, B.T., 2014. Soluble pathological tau in the entorhinal cortex leads to presynaptic deficits in an early Alzheimer's disease model. Acta Neuropathologica, 127(2), pp. 257-270.

PORTER, V.R., BUXTON, W.G., FAIRBANKS, L.A., STRICKLAND, T., O'CONNOR, S.M., ROSENBERG-THOMPSON, S. and CUMMINGS, J.L., 2003. Frequency and characteristics of anxiety among patients with Alzheimer's disease and related dementias. The Journal of Neuropsychiatry and Clinical Neurosciences, 15(2), pp. 180-186.

RABINOVICI, G.D., SEELEY, W.W., KIM, E.J., GORNO-TEMPINI, M.L., RASCOVSKY, K., PAGLIARO, T.A., ALLISON, S.C., HALABI, C., KRAMER, J.H., JOHNSON, J.K., WEINER, M.W., FORMAN, M.S., TROJANOWSKI, J.Q., DEARMOND, S.J., MILLER, B.L. and ROSEN, H.J., 2007. Distinct MRI atrophy patterns in autopsy-proven Alzheimer's disease and frontotemporal lobar degeneration. American Journal of Alzheimer's Disease and Other Dementias, 22(6), pp. 474-488.

RAMSDEN, M., KOTILINEK, L., FORSTER, C., PAULSON, J., MCGOWAN, E., SANTACRUZ, K., GUIMARAES, A., YUE, M., LEWIS, J., CARLSON, G., HUTTON, M. and ASHE, K.H., 2005. Age-dependent neurofibrillary tangle formation, neuron loss, and memory impairment in a mouse model of human tauopathy (P301L). The Journal of Neuroscience, 25(46), pp. 10637-10647.

RASCOVSKY, K., HODGES, J.R., KNOPMAN, D., MENDEZ, M.F., KRAMER, J.H., NEUHAUS, J., VAN SWIETEN, J.C., SEELAAR, H., DOPPER, E.G., ONYIKE, C.U., HILLIS, A.E., JOSEPHS, K.A.,

BOEVE, B.F., KERTESZ, A., SEELEY, W.W., RANKIN, K.P., JOHNSON, J.K., GORNO-TEMPINI, M.L., ROSEN, H., PRIOLEAU-LATHAM, C.E., LEE, A., KIPPS, C.M., LILLO, P., PIGUET, O., ROHRER, J.D., ROSSOR, M.N., WARREN, J.D., FOX, N.C., GALASKO, D., SALMON, D.P., BLACK, S.E., MESULAM, M., WEINTRAUB, S., DICKERSON, B.C., DIEHL-SCHMID, J., PASQUIER, F., DERAMECOURT, V., LEBERT, F., PIJNENBURG, Y., CHOW, T.W., MANES, F., GRAFMAN, J., CAPPA, S.F., FREEDMAN, M., GROSSMAN, M. and MILLER, B.L., 2011. Sensitivity of revised diagnostic criteria for the behavioural variant of frontotemporal dementia. Brain, 134(Pt 9), pp. 2456-2477.

RASCOVSKY, K., SALMON, D.P., HANSEN, L.A., THAL, L.J. and GALASKO, D., 2007. Disparate letter and semantic category fluency deficits in autopsy-confirmed frontotemporal dementia and Alzheimer's disease. Neuropsychology, 21(1), pp. 20-30.

ROBINSON, L., PLANO, A., COBB, S. and RIEDEL, G., 2013. Long-term home cage activity scans reveal lowered exploratory behaviour in symptomatic female Rett mice. Behavioural Brain Research, 250, pp. 148-156.

ROBINSON, L. and RIEDEL, G., 2014. Comparison of automated home-cage monitoring systems: emphasis on feeding behaviour, activity and spatial learning following pharmacological interventions. Journal of Neuroscience Methods, 234, pp. 13-25.

ROGERS, T.T., IVANOIU, A., PATTERSON, K. and HODGES, J.R., 2006. Semantic memory in Alzheimer's disease and the frontotemporal dementias: a longitudinal study of 236 patients. Neuropsychology, 20(3), pp. 319-335.

ROSENMANN, H., GRIGORIADIS, N., ELDAR-LEVY, H., AVITAL, A., ROZENSTEIN, L., TOULOUMI, O., BEHAR, L., BEN-HUR, T., AVRAHAM, Y., BERRY, E., SEGAL, M., GINZBURG, I. and ABRAMSKY, O., 2008. A novel transgenic mouse expressing double mutant tau driven by its natural promoter exhibits tauopathy characteristics. Experimental Neurology, 212(1), pp. 71-84.

RYAN, D., KOSS, D., PORCU, E., WOODCOCK, H., ROBINSON, L., PLATT, B. and RIEDEL, G., 2013. Spatial learning impairments in PLB1Triple knock-in Alzheimer mice are task-specific and age-dependent. Cellular and Molecular Life Sciences, 70(14), pp. 2603-2619.

SAHARA, N., DETURE, M., REN, Y., EBRAHIM, A.S., KANG, D., KNIGHT, J., VOLBRACHT, C., PEDERSEN, J.T., DICKSON, D.W., YEN, S.H. and LEWIS, J., 2013. Characteristics of TBS-extractable hyperphosphorylated tau species: aggregation intermediates in rTg4510 mouse brain. Journal of Alzheimer's Disease, 33(1), pp. 249-263.

SALOMONS, A.R., ARNDT, S.S. and OHL, F., 2012. Impact of anxiety profiles on cognitive performance in BALB/c and 129P2 mice. Cognitive, Affective & Behavioral Neuroscience, 12(4), pp. 794-803.

SALOMONS, A.R., BRONKERS, G., KIRCHHOFF, S., ARNDT, S.S. and OHL, F., 2010. Behavioural habituation to novelty and brain area specific immediate early gene expression in female mice of two inbred strains. Behavioural Brain Research, 215(1), pp. 95-101.

SANTACRUZ, K., LEWIS, J., SPIRES, T., PAULSON, J., KOTILINEK, L., INGELSSON, M., GUIMARAES, A., DETURE, M., RAMSDEN, M., MCGOWAN, E., FORSTER, C., YUE, M., ORNE, J., JANUS, C., MARIASH, A., KUSKOWSKI, M., HYMAN, B., HUTTON, M. and ASHE, K.H., 2005. Tau suppression in a neurodegenerative mouse model improves memory function. Science, 309(5733), pp. 476-481.

SCATTONI, M.L., GASPARINI, L., ALLEVA, E., GOEDERT, M., CALAMANDREI, G. and SPILLANTINI, M.G., 2010. Early behavioural markers of disease in P301S tau transgenic mice. Behavioural Brain Research, 208(1), pp. 250-257.

SCHINDOWSKI, K., BRETTEVILLE, A., LEROY, K., BEGARD, S., BRION, J.P., HAMDANE, M. and BUEE, L., 2006. Alzheimer's disease-like tau neuropathology leads to memory deficits and loss of functional synapses in a novel mutated tau transgenic mouse without any motor deficits. The American Journal of Pathology, 169(2), pp. 599-616.

SPITTAELS, K., VAN DEN HAUTE, C., VAN DORPE, J., BRUYNSEELS, K., VANDEZANDE, K., LAENEN, I., GEERTS, H., MERCKEN, M., SCIOT, R., VAN LOMMEL, A., LOOS, R. and VAN LEUVEN, F., 1999. Prominent axonopathy in the brain and spinal cord of transgenic mice overexpressing four-repeat human tau protein. The American journal of pathology, 155(6), pp. 2153-2165.

STOPFORD, C.L., THOMPSON, J.C., NEARY, D., RICHARDSON, A.M. and SNOWDEN, J.S., 2012. Working memory, attention, and executive function in Alzheimer's disease and frontotemporal dementia. Cortex, 48(4), pp. 429-446.

STOZICKA, Z., ZILKA, N., NOVAK, P., KOVACECH, B., BUGOS, O. and NOVAK, M., 2010. Genetic background modifies neurodegeneration and neuroinflammation driven by misfolded human tau protein in rat model of tauopathy: implication for immunomodulatory approach to Alzheimer's disease. Journal of Neuroinflammation, 7, pp. 64-2094-7-64.

TACKENBERG, C. and BRANDT, R., 2009. Divergent pathways mediate spine alterations and cell death induced by amyloid-beta, wild-type tau, and R406W tau. The Journal of Neuroscience, 29(46), pp. 14439-14450.

TAKEUCHI, H., IBA, M., INOUE, H., HIGUCHI, M., TAKAO, K., TSUKITA, K., KARATSU, Y., IWAMOTO, Y., MIYAKAWA, T., SUHARA, T., TROJANOWSKI, J.Q., LEE, V.M. and TAKAHASHI,

R., 2011. P301S mutant human tau transgenic mice manifest early symptoms of human tauopathies with dementia and altered sensorimotor gating. PloS one, 6(6), pp. e21050.

TANEMURA, K., AKAGI, T., MURAYAMA, M., KIKUCHI, N., MURAYAMA, O., HASHIKAWA, T., YOSHIIKE, Y., PARK, J.M., MATSUDA, K., NAKAO, S., SUN, X., SATO, S., YAMAGUCHI, H. and TAKASHIMA, A., 2001. Formation of filamentous tau aggregations in transgenic mice expressing V337M human tau. Neurobiology of Disease, 8(6), pp. 1036-1045.

TANEMURA, K., MURAYAMA, M., AKAGI, T., HASHIKAWA, T., TOMINAGA, T., ICHIKAWA, M., YAMAGUCHI, H. and TAKASHIMA, A., 2002. Neurodegeneration with tau accumulation in a transgenic mouse expressing V337M human tau. The Journal of Neuroscience, 22(1), pp. 133-141.

TARTAGLIA, M.C., HU, B., MEHTA, K., NEUHAUS, J., YAFFE, K., MILLER, B.L. and BOXER, A., 2014. Demographic and neuropsychiatric factors associated with off-label medication use in frontotemporal dementia and Alzheimer's disease. Alzheimer Disease and Associated Disorders, 28(2), pp. 182-189.

TATEBAYASHI, Y., MIYASAKA, T., CHUI, D.H., AKAGI, T., MISHIMA, K., IWASAKI, K., FUJIWARA, M., TANEMURA, K., MURAYAMA, M., ISHIGURO, K., PLANEL, E., SATO, S., HASHIKAWA, T. and TAKASHIMA, A., 2002. Tau filament formation and associative memory deficit in aged mice expressing mutant (R406W) human tau. Proceedings of the National Academy of Sciences of the United States of America, 99(21), pp. 13896-13901.

TERWEL, D., LASRADO, R., SNAUWAERT, J., VANDEWEERT, E., VAN HAESENDONCK, C., BORGHGRAEF, P. and VAN LEUVEN, F., 2005. Changed conformation of mutant Tau-P301L underlies the moribund tauopathy, absent in progressive, nonlethal axonopathy of Tau-4R/2N transgenic mice. The Journal of Biological Chemistry, 280(5), pp. 3963-3973.

VAN DER KOOIJ, M.A. and SANDI, C., 2012. Social memories in rodents: methods, mechanisms and modulation by stress. Neuroscience and Biobehavioral Reviews, 36(7), pp. 1763-1772.

VAN DER JEUGD, A., BLUM, D., RAISON, S., EDDARKAOUI, S., BUEE, L. and D'HOOGE, R., 2013. Observations in THY-Tau22 mice that resemble behavioral and psychological signs and symptoms of dementia. Behavioural Brain Research, 242, pp. 34-39.

VOGELSBERG-RAGAGLIA, V., BRUCE, J., RICHTER-LANDSBERG, C., ZHANG, B., HONG, M., TROJANOWSKI, J.Q. and LEE, V.M., 2000. Distinct FTDP-17 missense mutations in tau produce tau aggregates and other pathological phenotypes in transfected CHO cells. Molecular Biology of the Cell, 11(12), pp. 4093-4104.

WESSEL, J.R., ULLSPERGER, M., OBRIG, H., VILLRINGER, A., QUINQUE, E., SCHROETER, M.L., BRETSCHNEIDER, K.J., ARELIN, K., ROGGENHOFER, E., FRISCH, S. and KLEIN, T.A., 2015.

Neural synchrony indexes impaired motor slowing after errors and novelty following white matter damage. Neurobiology of Aging. [Ahead of Print]

WHITLOCK, J.R., HEYNEN, A.J., SHULER, M.G. and BEAR, M.F., 2006. Learning induces long-term potentiation in the hippocampus. Science, 313(5790), pp. 1093-1097.

YOSHIYAMA, Y., HIGUCHI, M., ZHANG, B., HUANG, S.M., IWATA, N., SAIDO, T.C., MAEDA, J., SUHARA, T., TROJANOWSKI, J.Q. and LEE, V.M., 2007. Synapse loss and microglial activation precede tangles in a P301S tauopathy mouse model. Neuron, 53(3), pp. 337-351.

ZAMBONI, G., HUEY, E.D., KRUEGER, F., NICHELLI, P.F. and GRAFMAN, J., 2008. Apathy and disinhibition in frontotemporal dementia: Insights into their neural correlates. Neurology, 71(10), pp. 736-742.

ZHANG, B., HIGUCHI, M., YOSHIYAMA, Y., ISHIHARA, T., FORMAN, M.S., MARTINEZ, D., JOYCE, S., TROJANOWSKI, J.Q. and LEE, V.M., 2004. Retarded axonal transport of R406W mutant tau in transgenic mice with a neurodegenerative tauopathy. The Journal of Neuroscience, 24(19), pp. 4657-4667.

Figure and Table Legends

Table1: Overview of transgenic hTau expressing mouse models. Model name, Tau mutation, isoform, promoter, expression level ('Expression'), regional expression ('Region'), histopathology and behavioural / cognitive phenotypes are shown, and listed in order of publication year. For onset, age in months is given either for earliest report of histopathology (a) or behaviour (b). For behavioural/cognitive phenotypes, specific aspects affected are given in brackets, arrows indicate decline or enhancement. Abbreviations: B.S. = brain stem, CaMKII = Ca2+/Calmodulin Kinase II, CNS = central nervous system, E.C = entorhinal cortex, EPM= elevated plus maze, Endo.= endogenous, F.B. = forebrain, L/D box =light/dark box, NFTs= neurofibrillary tangles, N.R. = not reported, OF =open field, P-Tau= phospho-Tau, PDGF-β=platelet-derived growth factor β, PrP= prion protein promotor, PPI= pre-pulse inhibition, S.C. = spinal cord , STFP = social transmission of food preference, Tet= Tetracycline inducible, WM= water maze. **[Table 1 – 2 column fit]**

Figure 1: $PLB2_{Tau}$ gene construct and transgene expression.

$PLB2_{Tau}$ mice were derived from $PLB1_{Double}$ mice expressing human *APP* and human *Tau*, crossed with Cre recombinase expressing mice. **A)** Genetic construct of $PLB1_{Double}$ mice: the CaMKIIα promoter, human APP_{770} gene (*hAPP*), an internal ribosome entry site (IRES) and the *human Tau 2N4R* gene (*hTau*) are shown. *hAPP* and *hTau* genes were flanked by LoxP and FRT excision sites, respectively. The $PLB2_{Tau}$ construct resulting from the crossing of $PLB1_{Double}$ mice with Cre recombinase mice is also depicted, where only the *hTau* gene remained. The product size of PCR amplification from a modified HPRT locus primer set is also illustrated. **B)** PCR confirmed the expression of the $PLB1_{Double}$ HPRT construct (5.2 kb) or the $PLB2_{Tau}$ HPRT construct (2.6 kb) in $PLB1_{Double}$ (PLB1) and $PLB2_{Tau}$ (PLB2) mice, respectively. PLB_{WT} and H_2O samples were included as negative controls. **C)** Regional transgene mRNA expression in 12-month old $PLB2_{Tau}$ forebrain and cerebellum samples were established by *hTau* specific RT-PCR. Predominant gene expression within the forebrain was confirmed. Mean data are expressed relative to the GAPDH house-keeping gene (+ SEM). ***=p<0.001. **[Figure 1 – 1 column fit]**

Figure 2: Tau protein expression in $PLB2_{Tau}$ mice.

A) Successful translation of the expressed hTau transgene was confirmed in heat-stable forebrain lysates from $PLB2_{Tau}$ mice (6 & 12-months of age) by immuno-blot detection. A single 60 kDa protein band (human specific HT-7 Tau antibody), was evident in all $PLB2_{Tau}$ mice lysates, in contrast no signal in PLB_{WT} was detected, despite endogenous Tau detection via the AT-5 Tau antibody. **B)** Quantification of hTau expression relative to total Tau at 6 and 12 months demonstrated a trend for an age-dependent decline in hTau levels ($p=0.07$). **C)** No overall increase of total Tau was observed relative to age-matched PLB_{WT} mice in both age groups. **D)** Individual analysis of each Tau (AT-5 positive) band revealed significant increases in the levels of 55 and 60 kDa Tau species in 6 month old $PLB2_{Tau}$ mice relative to PLB_{WT} controls ($n=14$ for both). **E)** Similar results were confirmed for $PLB2_{Tau}$ mice at 12 months of age. Data were normalised to either 6 months $PLB2_{Tau}$ samples for age comparison (B) or to age-matched PLB_{WT} mice (C-E) for total Tau expression and presented as mean +SEM. *=$p<0.05$ and **=$p<0.01$. **[Figure 2 – 2 column fit]**

Figure 3: Phospho-Tau expression in $PLB2_{Tau}$ mice.

A) Heat-stable forebrain lysates from PLB_{WT} and $PLB2_{Tau}$ mice (6- & 12-month of age) probed for PHF-1 phospho-Tau levels. **B)** Total PHF-1 positive Tau was increased at in both 6 and 12-month old $PLB2_{Tau}$ samples relative to age-matched controls. **C)** Significant elevations were detected at 55 and 50 kDa (bands analysed individually) in 6-month old $PLB2_{Tau}$ mice. **D)** By 12-month of age, the increase in PHF-1 phospho-Tau was more pronounced (all detected Tau bands) cf. $PLB1_{WT}$. **E)** Blots from lysates probed with CP-13. **F)** Elevated levels of total CP-13 phospho-Tau were detected in 6 and 12-month old $PLB2_{Tau}$ samples relative to age-matched controls. **G)** Individual analysis of CP-13 positive Tau bands demonstrated a selective increase of Ser202 phosphorylation of the 50 kDa Tau species in 6-month old $PLB2_{Tau}$ samples. **H)** Similar to PHF-1, phosphorylation levels increased with age, i.e. at 12 months significantly higher CP-13 signals were detected for all Tau bands (60, 55 & 50 kDa). **J)** An increase in AT-8 positive total Tau was detected at 6 and 12-months of age $PLB2_{Tau}$ samples, comprising of **K)** increased 50 kDa band AT-8 phosphorylation in 6-

month old $PLB2_{Tau}$ samples and **L)** increased AT-8 phosphorylation within 50 and 60 kDa bands in 12-month old $PLB2_{Tau}$ samples. All data were adjusted to total Tau expression prior to normalisation to age matched PLB_{WT} samples and are presented as means + SEM relative to WT (rel. to WT). *=p<0.05 and **=p<0.01, ***=p<0.001. **[Figure 3 – 2 column fit]**

Figure 4: Open field water maze: Intact acquisition and recall in $PLB2_{Tau}$ mice.

Spatial learning and recall abilities in PLB_{WT} and $PLB2_{Tau}$ mice were assessed in a standard open field water maze paradigm. **A)** At 6-months of age, $PLB2_{Tau}$ mice performed equivalent to age-matched PLB_{WT} mice during acquisition. **B)** Swim speed during acquisition was also unaffected. **C)** Both PLB_{WT} and $PLB2_{Tau}$ mice demonstrated retention for the trained platform position in the subsequent probe trial. **D)** 12-month old $PLB2_{Tau}$ mice were also not significantly affected during acquisition. **E)** However, a comparison of swim speeds demonstrated an accelerated rate for $PLB2_{Tau}$ mice relative to PLB_{WT} mice. **F)** Memory retention of platform position did not differ between groups at 12-month of age. Acquisition data and swim speed are expressed for each day (means ±SEM), and probe data is shown as % time in target quadrant (means +SEM). $ indicates statistical significance cf. chance level (p<0.05). **[Figure 4 – 1 column fit]**

Figure 5: Homecage spatial learning and reversal learning in $PLB2_{Tau}$ mice.

A*i*) No corner bias was observed during the habituation phase ('Habit') of the task (all corners supplying water) for either genotype. At 6-month old, PLB_{WT} mice displayed preference for the water supplying corner (% correct visits significantly above chance level) and thus retention for water access location during the 12 hr experimental phase (Test). $PLB2_{Tau}$ mice failed to attain significance. **A*ii)*** During a 12 hr reversal phase (Rev.), PLB_{WT} and $PLB2_{Tau}$ mice demonstrated a strong bias towards the water supplying corner, though notably $PLB2_{Tau}$ mice exhibited a weaker preference for the new location compared to PLB_{WT} mice. **B)** Total corner visits were reduced in $PLB2_{Tau}$ when compared to PLB_{WT} mice, in both **i)** the initial learning phase and **ii)** in reversal learning. **C)** At 12-month of age,

$PLB2_{Tau}$ mice failed to exhibit a corner preference during the spatial learning task in contrast to the intact corner learning of age matched PLB_{WT} mice. **D)** $PLB2_{Tau}$ mice again demonstrated reduced total corner visits at 12-month of age. Data are expressed as % correct corner visits (means + SEM) and total corner visits (means + SEM). $= $p<0.05$: comparison with chance level and *= $p<0.05$: comparison cf. PLB_{WT} controls. **[Figure 5 – 1 column fit]**

Figure 6: Social transmission of food preference in $PLB2_{Tau}$ mice.

Social interaction for cued food presentation was followed by either a short (15 mins; short-term memory [STM]) or long delay (24 hr; long-term memory [LTM]) prior to the mice being tested for recall via the presentation of correct and incorrect food. **A)** Analysis of food intake (g) demonstrated that PLB_{WT} mice consumed significantly more correct food (cued) during both STM and LTM tasks in comparison to incorrect food (non-cued), whereas $PLB2_{Tau}$ mice did not. **B)** When considered relative to total food consumed (%), $PLB2_{Tau}$ mice failed to demonstrate preference for cued food in either STM or LTM tasks, in contrast to age-matched PLB_{WT} mice. Data are presented as means + SEM. $= $p<0.05$ depicts significance vs. chance, *=$p<0.05$, **=$p<0.01$ and ***=$p<0.001$ is given for within-group comparisons or relative to WT's. **[Figure 6 – 1 column fit]**

Figure 7: Emotional behaviour of $PLB2_{Tau}$ mice.

At 6 months, $PLB2_{Tau}$ mice demonstrated heightened anxiety when assessed in the elevated plus maze (EPM). **A)** Relative to PLB_{WT} mice, $PLB2_{Tau}$ mice spent an increased amount of time (%) in the closed arms and less time within the open arms of the apparatus.

The hedonistic motivation / pleasure seeking behaviour of $PLB2_{Tau}$ mice was assessed by a 3-day sucrose preference test **(B). Bi)** PLB_{WT} mice demonstrated a clear preference for sucrose over untreated water on all days (%), $PLB2_{Tau}$ mice failed to display a preference for sucrose on day 1, only discriminating for sucrose solution on days 2 and 3. **Bii)** Lick data for water and sucrose over the 3 days of testing confirmed that both PLB_{WT} and $PLB2_{Tau}$ mice presented with an overall preference for sucrose. However, $PLB2_{Tau}$ mice performed fewer

sucrose licks and increased water licks when compared with WT's. Data are illustrated as % time in zones, % sucrose corner visits and % licks (mean +SEM), $= p<0.05 indicates results relative to chance level, *=p<0.05 **=p<0.01 and ***=p<0.001 depicts differences between $PLB2_{Tau}$ and PLB_{WT} mice. **[Figure 7 – 2 column fit]**

Figure 8: Intact motor function of $PLB2_{Tau}$ mice.

The motor performance of 14-month old PLB_{WT} and $PLB2_{Tau}$ mice was assessed in the balance beam paradigm and quantified as latency to traverse **A)** square or **B)** round beams of various diameters (5, 11 and 28 mm). No motor deficits were observed in $PLB2_{Tau}$ mice compared to PLB_{WT} in either of the tests. Note the slight improvement in the latency of $PLB2_{Tau}$ mice apparent for the 28 mm square beam test. Data are presented as mean time (in seconds) ± SEM. *=p<0.05 refers to results from a Bonferroni multiple comparisons post-test. **[Figure 8 – 1 column fit]**

Figure 9: Habituation to a novel environment, exploratory activity and circadian rhythm in $PLB2_{Tau}$ mice.

A) Non-linear regression of exploratory activity (for mean distance moved [cm], 10 min bins) during the 3 hr habituation phase indicated lower activity in 6-month old $PLB2_{Tau}$ when compared to PLB_{WT} mice. **B)** Reduced ambulatory activity of $PLB2_{Tau}$ mice was also evident over the following 4 days (mean distance moved, 1hr bins) and when pooled across the 96 hr observation period (**C**). Basic circadian activity was maintained in $PLB2_{Tau}$ mice, with a decreased activity observed for data pooled during light and dark phases (**D)**. Data are shown as mean distance moved ± or + SEM. **=p<0.01. **[Figure 9 – 2 column fit]**

Figure 10: Vigilance stage composition and EEG power spectra of $PLB2_{Tau}$ mice.

A) $PLB2_{Tau}$ mice spent an increased time awake (wakefulness, W) cf. PLB_{WT} mice, which corresponded to a reduction in NREM (NR) sleep during the midday recording period (4 hrs), without alterations in REM (R) occurrence. Recordings during the midnight period did not reveal significant difference in vigilance stage composition. **B)** Corresponding stage-

specific EEG spectra (pooled per group and vigilance stage from the 8 hrs data set) demonstrated stage- and region-specific alterations. Data are expressed as means +SEM (A) and means ±SEM (B). Overall effects of genotype and interactions are reported on the right, band-specific genotype effects (*) and interactions ($) are also indicated as */$=p<0.05 **/$$=p<0.01 and ***/$$$=p<0.001. **[Figure 10 – 2 column fit]**

Figure 11: Hippocampal slice physiology in $PLB2_{Tau}$ mice.

Basic synaptic transmission and LTP were assessed in hippocampal slices from 6, 12 and 24 months old $PLB2_{Tau}$ and PLB_{WT} mice. IO curves of synaptic transmission are shown as fEPSP slope in relation to **(A)** stimulus intensity [stim. intensity] and **(B)** presynaptic fibre volley. When considered as a function of stimulus intensity, synaptic transmission was only affected in 24 months old $PLB2_{Tau}$ mice relative to PLB_{WT} mice. In contrast, fEPSP slope plotted relative to the presynaptic fibre volley demonstrated a robust decrease in synaptic efficiency in all age groups of $PLB2_{Tau}$ mice compared to PLB_{WT} mice. **C)** Hippocampal CA1 LTP was overall unaffected in all age groups of $PLB2_{Tau}$ mice, though a trend for decreased potentiation was observed at 12 months cf. PLB_{WT} controls. Data are expressed as mean fEPSP slope +SEM for IO curves and as fEPSP slope (% of pre-tetanus baseline) +SEM for LTP. ***=p<0.001. **[Figure 11 – 2 column fit]**

Figure1

Click here to download high resolution image

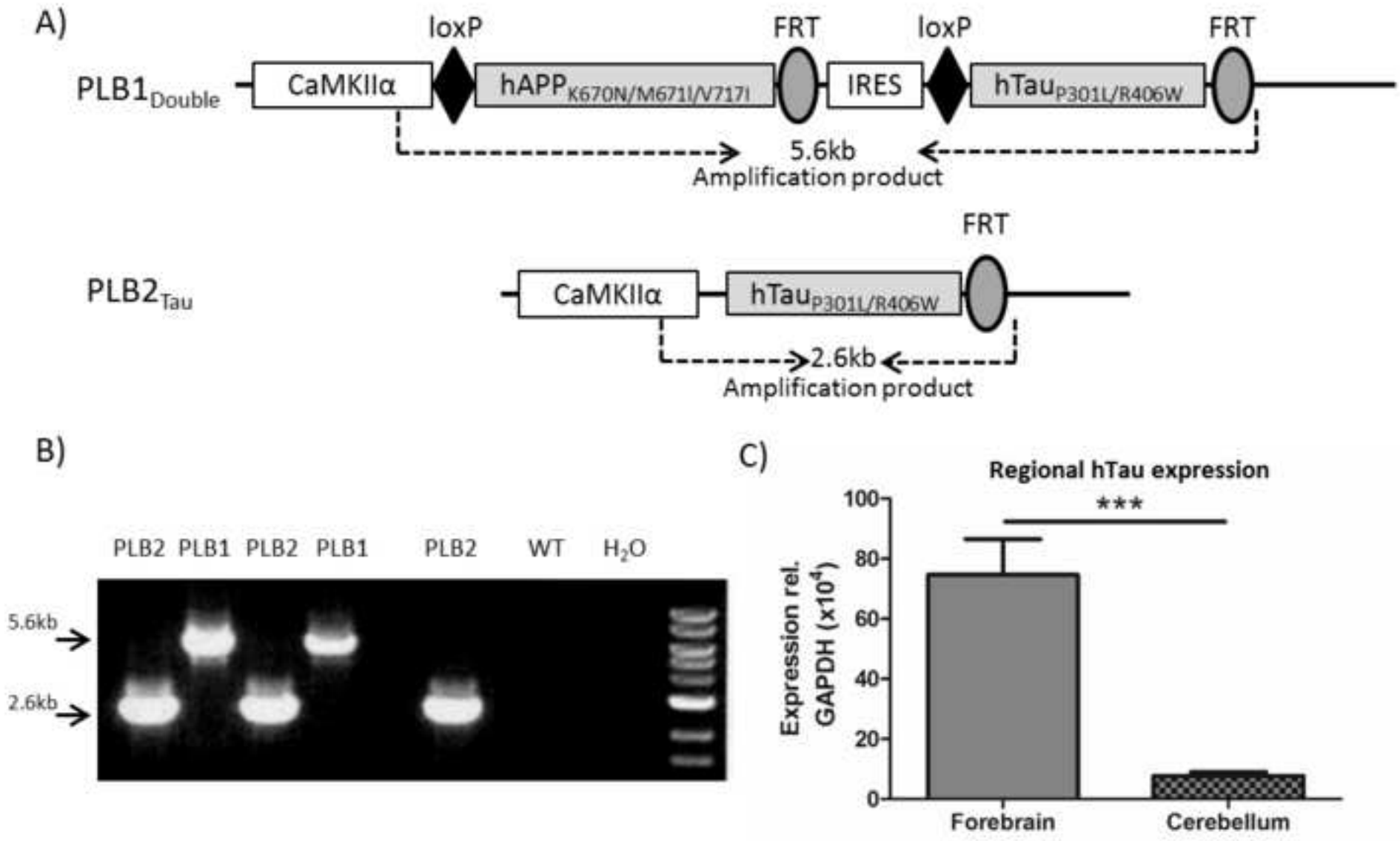

Figure2

Click here to download high resolution image

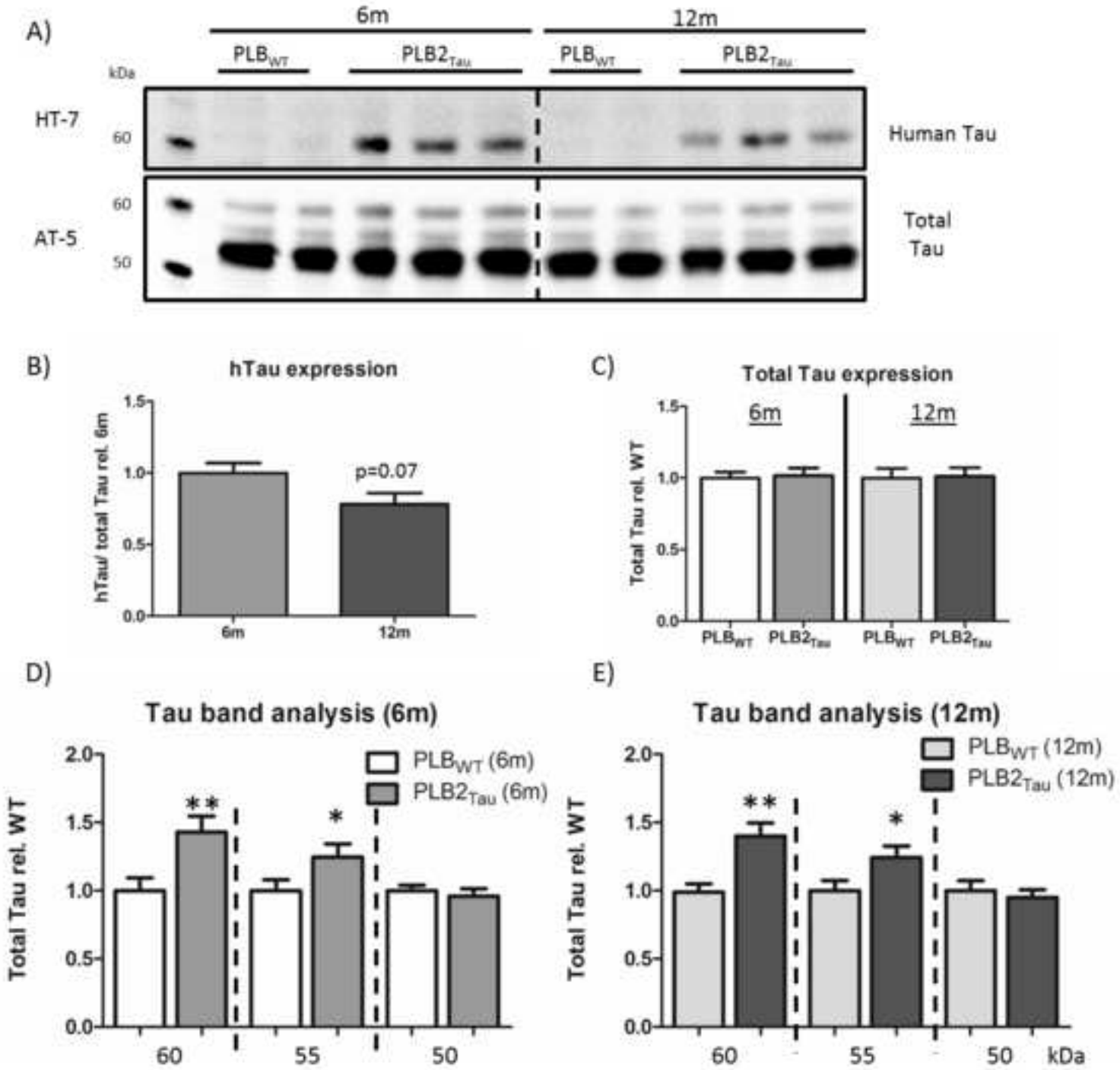

Figure 3 (revised)

Click here to download high resolution image

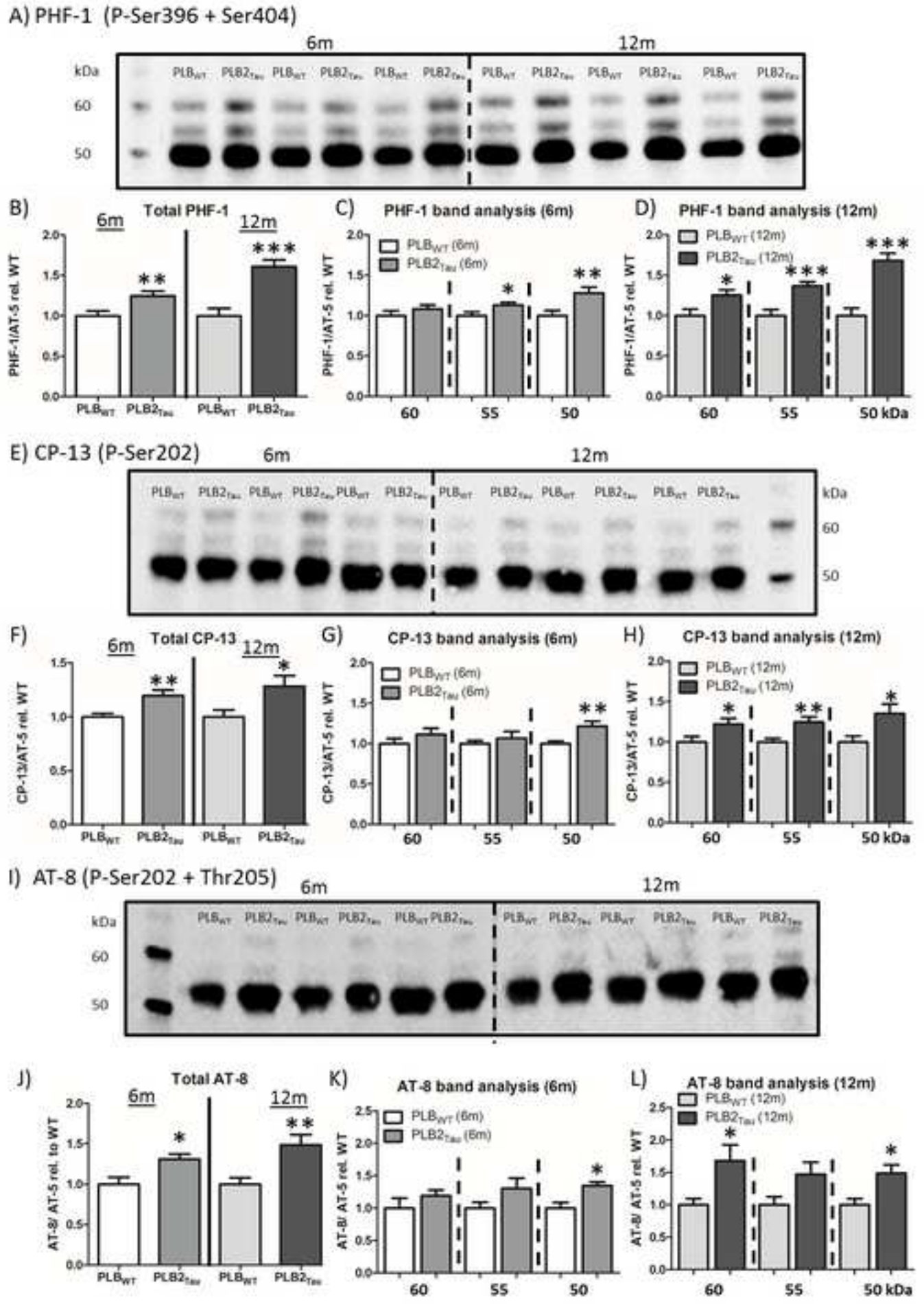

Figure4

Click here to download high resolution image

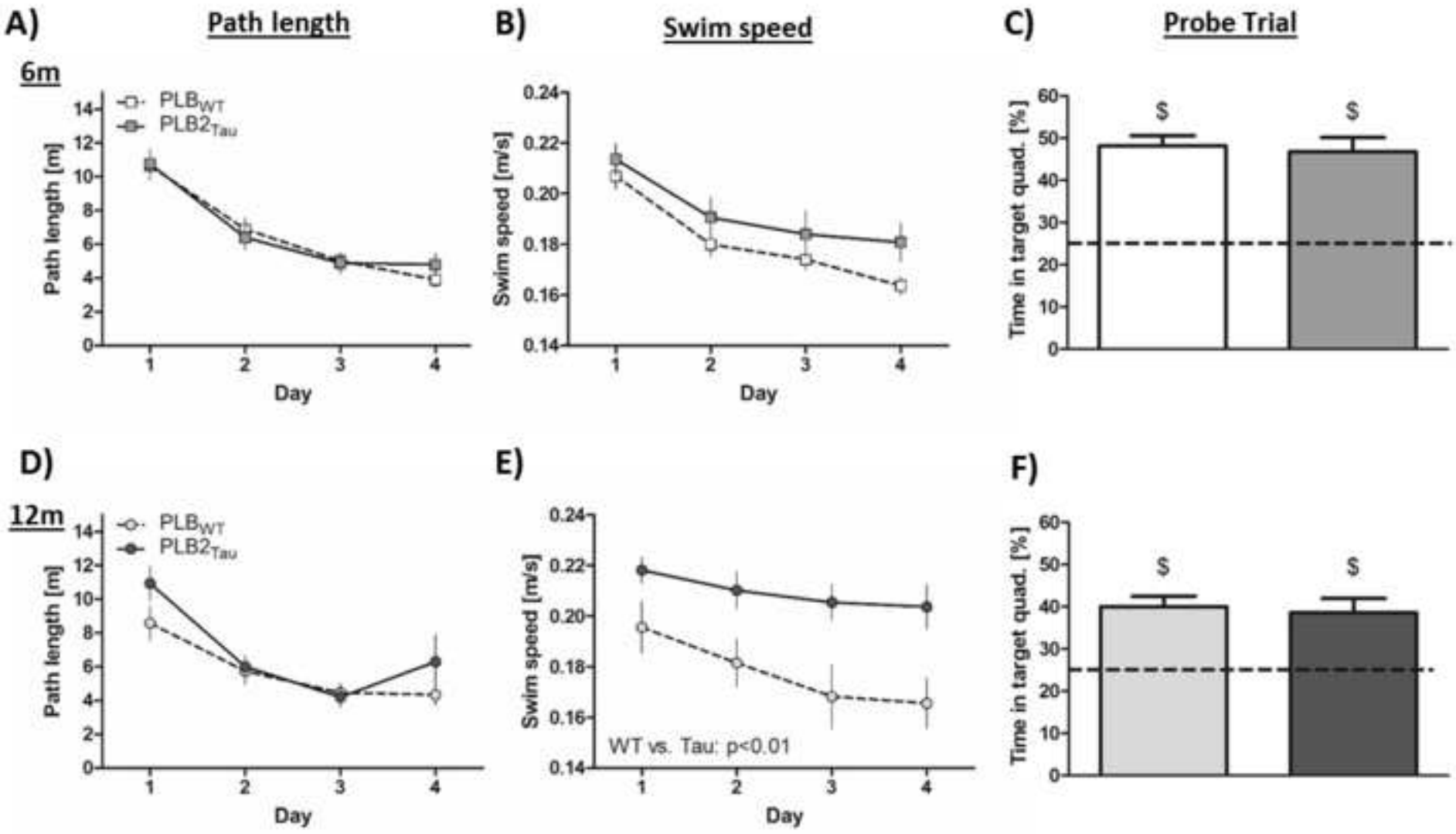

Figure5

Click here to download high resolution image

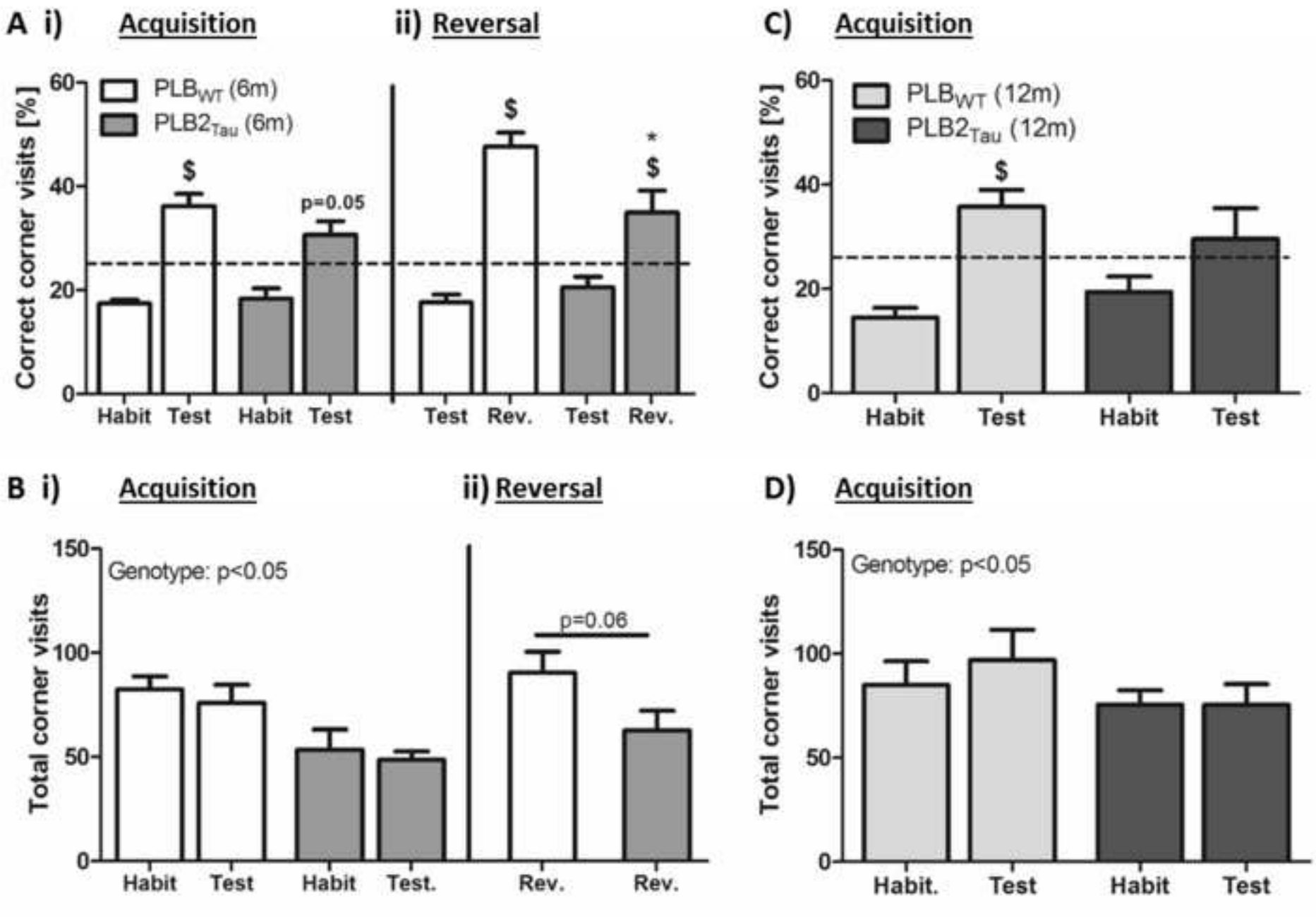

Figure6
Click here to download high resolution image

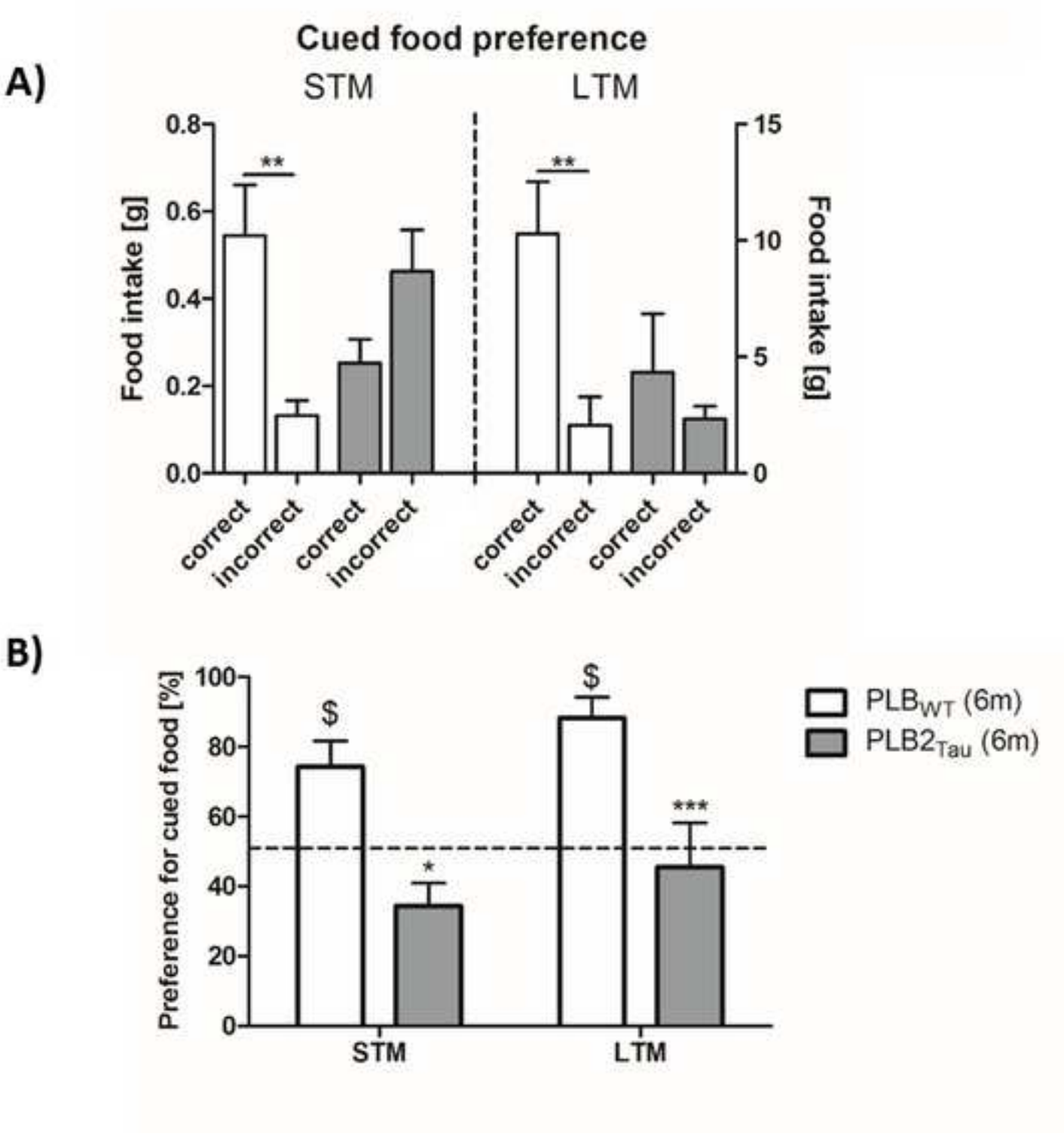

Figure7

Click here to download high resolution image

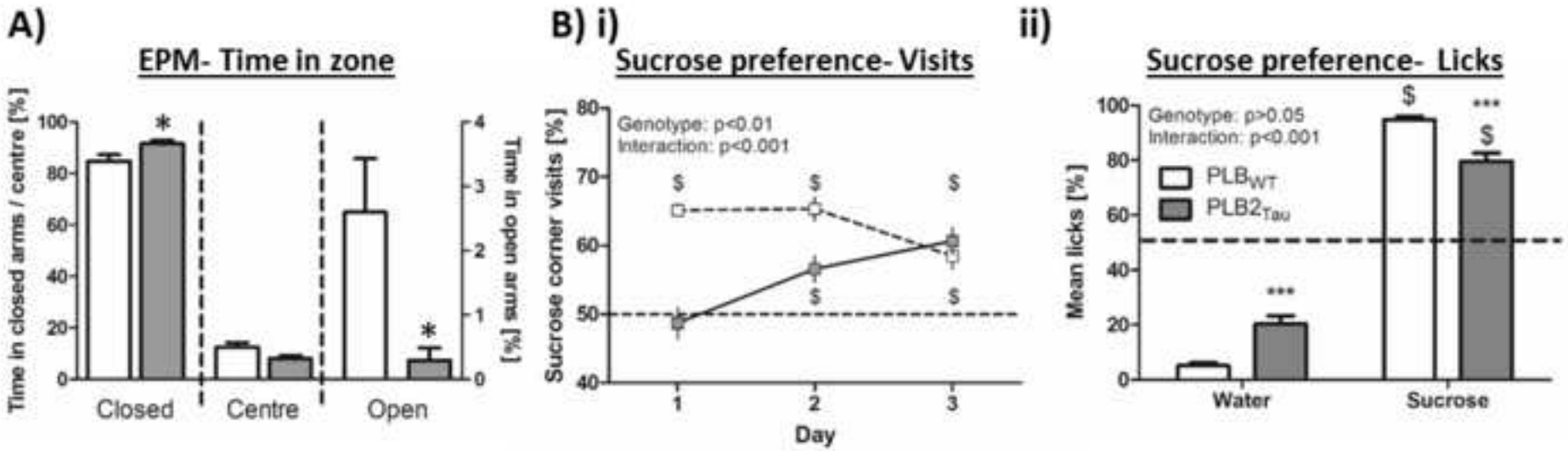

Figure8

Click here to download high resolution image

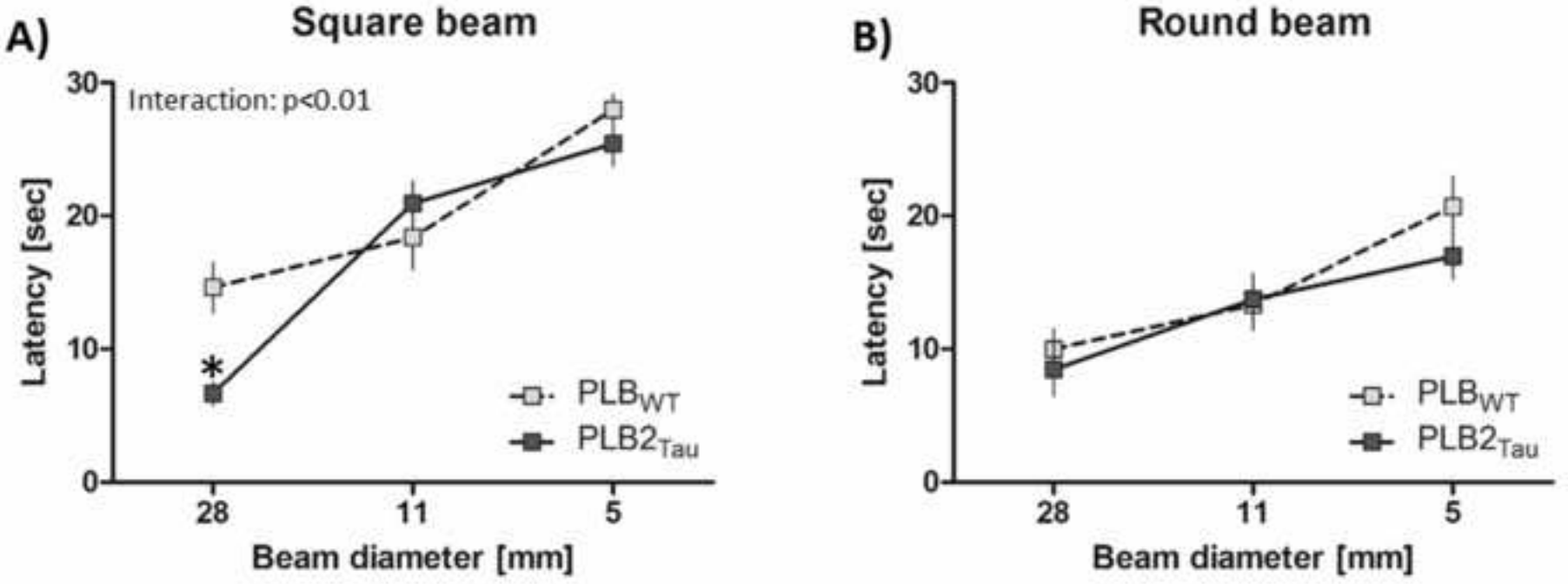

Figure9

Click here to download high resolution image

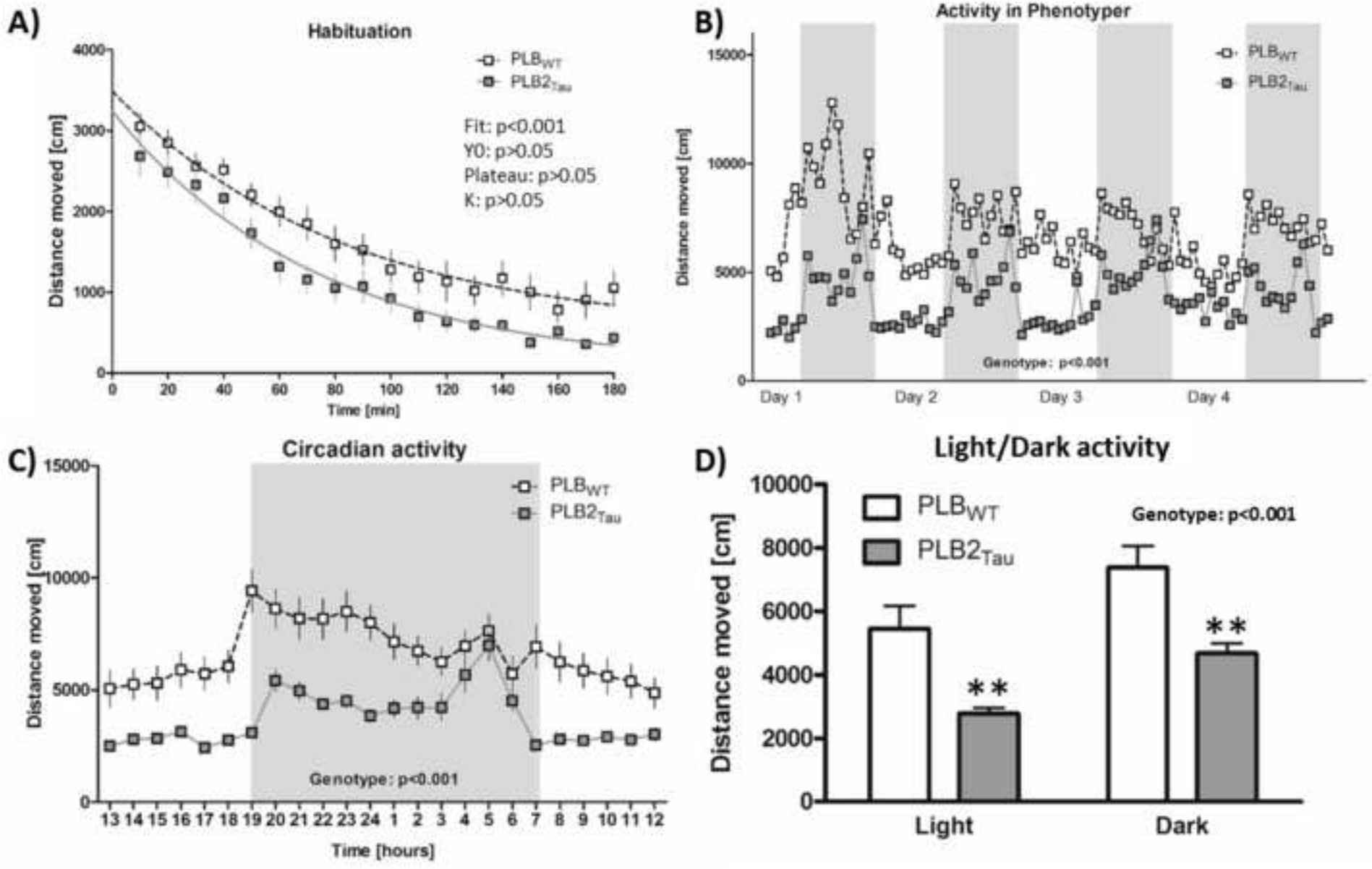

Figure10

Click here to download high resolution image

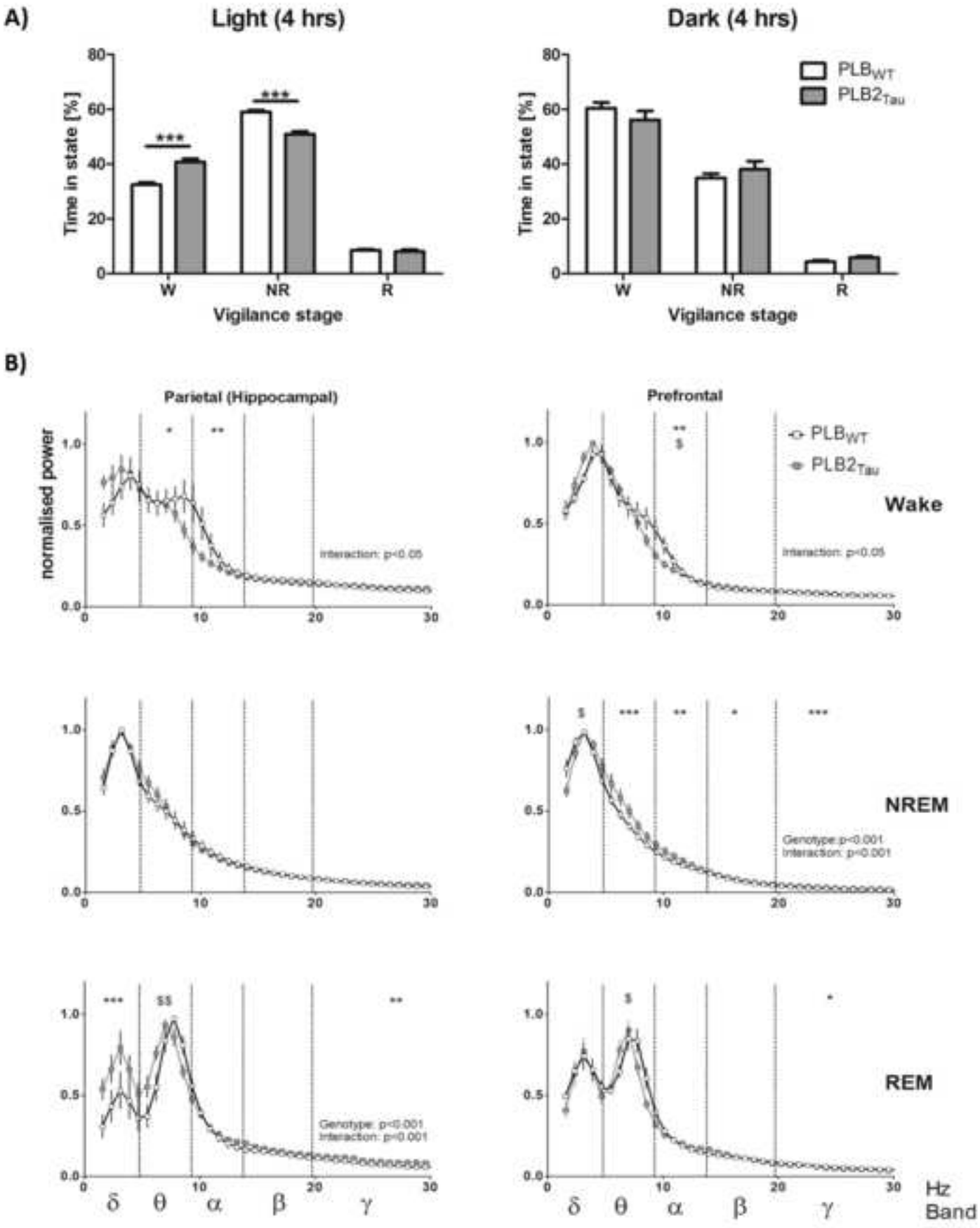

Figure11

Click here to download high resolution image

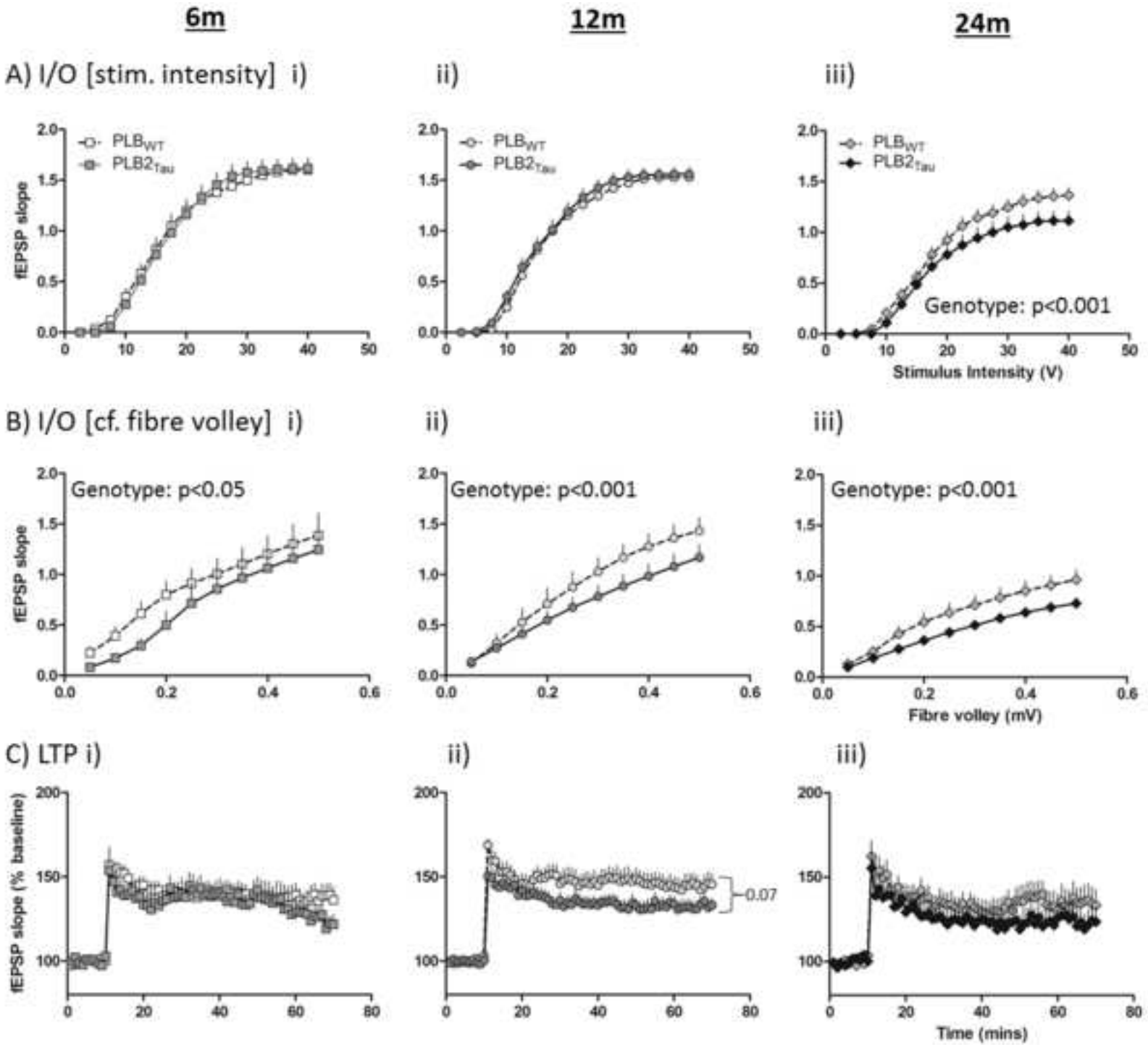

Table 1

Tau variant (name)	Iso-form	Pro-moter	Expression (fold)	Region	Onset (m)	Histopathology	Behavioural /cognitive phenotype	Reference
P301L (JNPL3)	4R2N	mPrP	2	CNS + S.C.	4[b]	P-Tau / NFTs in F.B .+ S.C. + B.S. Spinal motor neuron loss (>8m)	Motor deficits	Lewis et al., 2000
P301L	4R2N	Thy 1.2	N.R.	CNS + S.C.	3[a]	P-Tau / NFT in F.B. + S.C. + B.S.	No motor deficit	Gotz et al., 2001
V337M	4R2N	PDGF-β	0.1	CNS: F.B	12[b]	P-Tau / NTFs in F.B.	No WM deficit Increase in EPM open arms (↓anxiety)	Tanemura et al., 2001 +2002
P301S	4R0N	Thy 1	2	CNS + S.C.	3[b]	P-Tau / NFTs in F.B .+ S.C. Spinal neuron loss Muscle atrophy	Motor deficits WM deficits (↓memory) Increased time in OF centre (↓anxiety)	Allen et al., 2002 Scattoni et al., 2010
R406W	4R2N	CaMKII	0.2	CNS: F.B	16[b]	P-Tau / NFTs in F.B.	No motor deficits Cued/Contextual fear conditioning (↓memory) No difference in L/D box (−anxiety) PPI deficits (↑psychosis) Immobility in forced swim test (↑depression)	Tatebayash et al., 2002 Egashira et al., 2005
R406W	4R2N	mPrP	10	CNS + S.C.	2[a]	P- Tau / NFTs in F.B .+ S.C.	N.R.	Zhang et al., 2004
P301L (Tg4510)	4R0N	CaMKII (Tet)	13	CNS: F.B	2-4[b]	P-Tau / NFTs in F.B. Cortico-spinal neuron loss (>10m)	Motor deficits WM deficits (↓memory) Contextual fear conditioning (↓memory) PPI deficits (↑psychosis)	SantaCruz et al., 2005 Ramsden et al., 2005 Hunsburger et al.,2014 Koppel et al., 2014
P301S+ G227V (THY-Tau22)	4R1N	Thy 1.2	5	CNS + S.C.	3[b]	P-Tau /NFTs in F.B.	No motor deficits WM deficit (↓memory) STFP deficit (↓memory) Y-maze deficit (↓memory) contextual fear conditioning (↓memory) Increase in EPM open arms (↓anxiety) immobility in tail suspension test (↑depression) Reduced reward performance (↑anhedonia)	Schindowski et al., 2006 Van der Jeugd et al., 2011+ 2013
P301S (PS19)	4R1N	mPrP	5	CNS + S.C.	3[b]	P-Tau / NFTs in F.B. + S.C. Spinal neuron loss Muscle atrophy	Motor deficits WM deficits (↓memory) Increase in EPM open arms (↓anxiety) PPI deficits (↑psychosis) Decreased hot plate threshold (↑nociception) No change in forced swim test	Yoshiyama et al., 2007 Takeuchi et al., 2011
K257T +P301S (DM Tau-tg)	4R0N	Tau	0.1	CNS + S.C	6[b]	P-Tau and NFTs in F.B.	No motor deficits WM deficits (↓memory) RAWM deficits (↓memory)	Rosenmann et al., 2008
P301L (rTg TauEC)	4R0N	CAMKII / neuropsin	N.R	E.C hippocampus	3[a]	P-Tau and NFTs in E.C and hippocampus Propagation of pathology via synaptic connections	Contextual fear conditioning deficit (↓memory)	De Calignon et al., 2012 Polydoro et al., 2014
P301L (P301L KI)	All Endo	Tau	0	CNS + S.C	N.A	Tau hypophosphorylation No NFTs Reduced Microtubule association Mitochondria transport abnormalities	No motor deficits No deficits in STFP Enhanced locomotion	Gilley et al., 2012
V337M + R406W (TMHT)	4R2N	mThy-1	2	CNS	5[b]	P-Tau /NFTs in F.B.	No motor deficits WM deficits (↓memory) Immobility forced swim test (↑depression) Impairment in buried cookie test (↓olfaction)	Flunkert et al., 2013
P301S+ G335D (Line 66)	4R2N	mThy-1	2	CNS	6[b]	P-Tau/NFTs in F.B.	Motor deficits No WM deficit Reduced thigmotaxis (↓anxiety)	Melis et al., 2015